Analytical $O(\alpha_s)$ corrections to the beam frame double-spin density matrix elements of $e^+e^- \to t\bar{t}$

L. Kaldamäe,[1] S. Groote,[1] and J. G. Körner[2]

[1]*Loodus- ja Tehnoloogiateaduskond, Füüsika Instituut, Tartu Ülikool, W. Ostwaldi 1, 50411 Tartu, Estonia*

[2]*PRISMA Cluster of Excellence, Institut für Physik, Johannes-Gutenberg-Universität, Staudinger Weg 7, 55099 Mainz, Germany*

We provide analytical results for the $O(\alpha_s)$ corrections to the double-spin density matrix elements in the reaction $e^+e^- \to t\bar{t}$. These concern the elements ll, lt, ln, tt, tn, and nn of the double-spin density matrix elements where l, t, n stand for longitudinal, transverse and normal orientations with respect to the beam frame spanned by the electron and the top quark momentum.

I. INTRODUCTION

The measurement of polarization effects in top and antitop quark events produced at e^+e^- colliders is very interesting in that one can test the details of the Standard Model production and decay mechanisms of the produced top-antitop quark pairs and their decays. In addition such measurements can be used to constrain deviations from Standard Model couplings [1–4]. While single-spin polarization effects are not observed for hadronically produced top quark pairs as at the LHC due to parity conservation [5], single-spin polarization effects are present in e^+e^- colliders due to the existence of parity-violating components in the production mechanism [6]. Parity conservation in the production mechanism for the top and antitop pair, however, allows for spin-spin correlation effects between top and antitop quark spins as at the LHC. The analysis of spin-spin correlations of top quark pairs has become a very popular subject in the last few years (see e.g. Ref. [7]).

The top quark retains its polarization at birth when it decays because its lifetime is so short that it decays before hadronization can wash out its polarization. Therefore, polarization effects at the envisaged e^+e^- colliders ILC and CLIC should help to find new physics. Of interest is also the role of quark mass effects in the production of quarks and gluons in e^+e^- annihilations. Analytical results for the $O(\alpha_s)$ radiative corrections to longitudinal single-spin polarization including quark mass effects can be found in Refs. [8–12], and corresponding results for the transverse and normal polarization components can be found in Ref. [13]. In Refs. [14–16] analytical results for the $O(\alpha_s)$ radiative corrections to longitudinal spin-spin correlations between massive quark pairs can be found.

The aim of this paper is twofold. On the one hand we provide an independent check of the numerical next-to-leading-order (NLO) results presented in Refs. [17,18]. On the other hand we provide analytical results for the $O(\alpha_s)$ radiative corrections to the transverse and transverse normal spin-spin correlation asymmetry (called transverse and normal spin-spin asymmetry for short) and its polar angle dependence for massive quark pairs produced in e^+e^- annihilations.

To define and measure single-spin and spin-spin correlation observables requires the definition of one or two coordinate systems in the top quark and antitop quark rest systems. Several coordinate bases have been proposed in Ref. [19], namely the helicity basis, beamline basis and off-diagonal basis. As advised in Refs. [17,18], in this paper we use a common basis for both top and antitop quark observables. As the z direction lies along the direction of the top quark, for the top quark this basis can be referred to as the helicity basis. However, two linearly independent directions are necessary to build a frame. The beam frame used here is spanned by the momenta of the electron and quark. Leading-order results for spin-spin correlations in this frame have been given in Ref. [19] while numerical results for the $O(\alpha_s)$ radiative corrections can be found in Refs. [17,18]. However, it is not really necessary to choose a common reference frame for the top and antitop rest frames. For example, in Refs. [15,16,20] the respective helicity systems for the top and antitop were chosen which are not necessarily anticollinear at NLO. Still, the differences are marginal because the mean deviation from the anticollinearity due to $O(\alpha_s)$ corrections is small [21].

In performing these calculations in the beam frame spanned by the momenta of the electron and the quark, it turned out that the integrals necessary for the phase space integration are quite similar to those used by us in former calculations [8–16] (see also Ref. [22] for the mathematical background). Calculations performed in the event frame spanned by the top, antitop and gluon including also elliptic integrals will be found in a separate publication [23].

In the course of this paper we also explain how to measure the spin-spin correlation (see e.g. Refs. [24,25]). As in the corresponding hadronic case [26–29] we investigate spin-spin correlation effects through

(1) the double angle distribution[1]

$$\frac{1}{\sigma}\frac{d\sigma}{d\cos\theta_1 d\cos\theta_2}$$
$$= \frac{1}{4}(1 + B_1\cos\theta_1 - B_2\cos\theta_2 - C\cos\theta_1\cos\theta_2),$$

$$(1)$$

where θ_1 and θ_2 are the angles between a fixed direction given by the basis used and the direction of flight of the charged lepton in the rest frames of the top and antitop quark, respectively, and

(2) the opening angle distributions

$$\frac{1}{\sigma}\frac{d\sigma}{d\phi} = \frac{1}{4}(1 - D\cos\phi),$$

$$(2)$$

where ϕ is the angle between the directions of flight of the charged leptons in the rest frames of the top and antitop quark, respectively.

In Refs. [26–29] Bernreuther and coworkers dealt with the subject of top-antitop spin-spin correlations at hadron colliders. They introduced a variety of spin-spin observables and gave detailed prescriptions of how to measure these observables.

The paper is organized as follows. In Sec. II we deal with the double-spin density matrix, we specify quantization axes and introduce observables. In addition, we explain how these observables are related to angular dependences measured in subsequent particle cascades. In Sec. III we introduce our analytical $O(\alpha_s)$ results which are found in Appendices A and B. The dependence of the observables on the center-of-mass energy, the polar angle and the initial beam polarization are discussed in Sec. IV. Section V contains our conclusions.

II. THE DOUBLE-SPIN DENSITY MATRIX

Polarization observables are best described in terms of the spin density matrix. The two spin states of a spin-1/2 fermion are denoted by $|\lambda = \pm 1/2\rangle$. The two spin states are eigenstates of the spin operator J_z in a given frame. The coefficients of the normalized spin density matrix $\hat{\rho}$ are given by superpositions of the elements $|\lambda\rangle\langle\lambda'|$. In a moving frame one has the completeness relation

$$\not{p} + m_f = \sum_{\lambda=\pm 1/2}|\lambda\rangle\langle\lambda|.$$

$$(3)$$

One can represent the two spin states as components of a two-dimensional Pauli spinor which implies that one can parametrize the (normalized) spin density matrix in terms of Pauli matrices according to[2]

$$\hat{\rho} = (\hat{\rho}_{\lambda,\lambda'}) = \frac{1}{2}(\mathbb{1} + P^i\hat{\sigma}_i),$$

$$(4)$$

where $\vec{P} = (P^i)$ is the three-dimensional polarization vector. The expectation value of an arbitrary operator $\mathcal{O}$ is obtained by calculating the trace, $\langle\mathcal{O}\rangle = \text{Tr}(\hat{\rho}\mathcal{O})$.

Next we introduce the double-spin density matrix which is needed for the discussion of spin-spin correlation effects. Given a quantization axis for the observation of single-spin polarization and spin-spin correlation effects in e^+e^- collisions, the 4×4 un-normalized double density matrix $\hat{\rho}$ is parametrized by expanding the density matrix along outer products of the standard set of 2×2 matrices. One has

$$\hat{\rho} = (\hat{\rho}_{\lambda_1\lambda_2,\lambda'_1\lambda'_2})$$
$$= \frac{1}{4}(\rho\mathbb{1} \otimes \mathbb{1} + \rho^{e^i_1}\hat{\sigma}_i \otimes \mathbb{1} + \rho^{\bar{e}^j_2}\mathbb{1} \otimes \hat{\sigma}_j + \rho^{e^i_1\bar{e}^j_2}\hat{\sigma}_i \otimes \hat{\sigma}_j)$$

$$(5)$$

where the outer product symbol $\otimes$ denotes the tensor product between the spin states of the top and antitop quarks according to $(A\otimes B)_{\lambda_1\lambda_2,\lambda'_1\lambda'_2} = A_{\lambda_1\lambda'_1}B_{\lambda_2\lambda'_2}$. The labels λ_1 (λ'_1) and λ_2 (λ'_2) denote the two spin states of the top and antitop quark, respectively.

A. Quantization axes

Given a quantization axis for each spin degree of freedom represented by the two orientation vectors $\vec{e}_1$ and $\vec{\bar{e}}_2$, the coefficient functions ρ, $\rho^{e^i_1}$, $\rho^{\bar{e}^j_2}$ and $\rho^{e^i_1\bar{e}^j_2}$ denoting the rate function, the un-normalized single-spin polarization components of the top and antitop quarks, and the double-spin correlation component, respectively, can be projected from Eq. (5) by tracing the appropriate products of $\hat{\rho}$ with $\mathbb{1} \otimes \mathbb{1}$, $e^i_1\hat{\sigma}_i \otimes \mathbb{1}$, $\bar{e}^j_2\mathbb{1} \otimes \hat{\sigma}_j$ or $e^i_1\bar{e}^j_2\hat{\sigma}_i \otimes \hat{\sigma}_j$. One obtains

$$\rho = \rho(\uparrow,\uparrow) + \rho(\uparrow,\downarrow) + \rho(\downarrow,\uparrow) + \rho(\downarrow,\downarrow),$$
$$\rho^{e_1} = \rho(\uparrow,\uparrow) + \rho(\uparrow,\downarrow) - \rho(\downarrow,\uparrow) - \rho(\downarrow,\downarrow),$$
$$\rho^{\bar{e}_2} = \rho(\uparrow,\uparrow) - \rho(\uparrow,\downarrow) + \rho(\downarrow,\uparrow) - \rho(\downarrow,\downarrow),$$
$$\rho^{e_1\bar{e}_2} = \rho(\uparrow,\uparrow) - \rho(\uparrow,\downarrow) - \rho(\downarrow,\uparrow) + \rho(\downarrow,\downarrow)$$

$$(6)$$

where $\uparrow$ and $\downarrow$ represent the two orientations with respect to the quantization axes. For the production process $e^+e^- \to t\bar{t}(G)$, the contributions on the right-hand side of Eq. (6) are given by

---

[1]For hadronically produced top-antitop quark pairs the single angle coefficients B_1 and B_2 vanish at LO due to parity conservation of the strong interactions.

[2]In order to distinguish between the Pauli matrix and cross section, we use the symbol $\hat{\sigma}$ for the former.

$$\rho(\vec{s}_1, \vec{s}_2) = \text{Tr}\left(\hat{\rho}\,\frac{1}{2}(\mathbb{1} + \vec{s}_1 \cdot \hat{\sigma}) \otimes \frac{1}{2}(\mathbb{1} + \vec{s}_2 \cdot \hat{\sigma})\right)$$

$$= \frac{e^4 N_c}{q^4} \sum_{i,j=1}^{4} g_{ij} L^i_{\mu\nu} H^{j\mu\nu} = |T_{fi}|^2 \qquad (7)$$

defining the spin dependence of the squared matrix element $|T_{fi}|^2$ of the production process, where q is the momentum carried by the intermediate boson (γ or Z). The multi-component overall factor $e^4 N_c g_{ij}/q^4$ incorporates the boson propagator effect and the multicomponent electroweak coupling factors g_{ij} which includes the dimensionless part of the interactions of the fermions with the bosons (cf. Ref. [12]). The various components of the lepton tensor $L^i_{\mu\nu}$ and hadron tensor $H^i_{\mu\nu}$ are decomposed according to

$$L^1 = \frac{1}{2}(L^{VV} + L^{AA}), \qquad L^2 = \frac{1}{2}(L^{VV} - L^{AA}),$$

$$L^3 = \frac{i}{2}(L^{VA} - L^{AV}), \qquad L^4 = \frac{1}{2}(L^{VA} + L^{AV}) \qquad (8)$$

(and accordingly for the H^i) where V and A denote the vector and axial-vector contributions. The double density matrix can now be expanded into the tensor product of two bases. In Ref. [17] the directions of the top quark ($\hat{k}$), the electron momentum ($\hat{p}$) and a normalized vector ($\hat{n}$) perpendicular to these two has been used for both bases. These two bases need not be the same. For convenience of the phenomenological calculation of the double density matrix via $\rho(\vec{s}_1, \vec{s}_2)$, we choose as bases the bases $(\vec{s}_i^T, \vec{s}_i^N, \vec{s}_i^L)$ of the two spins s_i ($i = 1, 2$) boosted to the laboratory frame. The respective rest frame spin vectors are given by

$$\vec{s}_1^T = (1, 0, 0), \qquad \vec{s}_1^N = (0, 1, 0), \qquad \vec{s}_1^L = (0, 0, 1),$$
$$\vec{s}_2^T = (\cos\theta_{12}, 0, -\sin\theta_{12}), \qquad \vec{s}_2^N = (0, 1, 0),$$
$$\vec{s}_2^L = (\sin\theta_{12}, 0, \cos\theta_{12}), \qquad (9)$$

where θ_{12} is the polar angle between the momenta of the top and antitop quarks. At the Born term level one has $\theta_{12} = \pi$. One obtains the double expansion

$$\hat{\rho} = \frac{1}{4}\Big(\rho(\mathbb{1} \otimes \mathbb{1}) + (\rho^T s_1^{iT} + \rho^N s_1^{iN} + \rho^L s_1^{iL})(\hat{\sigma}_i \otimes \mathbb{1})$$
$$+ (\rho^{\bar{T}} s_2^{jT} + \rho^{\bar{N}} s_2^{jN} + \rho^{\bar{L}} s_2^{jL})(\mathbb{1} \otimes \hat{\sigma}_j)$$
$$+ (\rho^{T\bar{T}} s_1^{iT} s_2^{jT} + \rho^{T\bar{N}} s_1^{iT} s_2^{jN} + \rho^{T\bar{L}} s_1^{iT} s_2^{jL}$$
$$+ \rho^{N\bar{T}} s_1^{iN} s_2^{jT} + \rho^{N\bar{N}} s_1^{iN} s_2^{jN} + \rho^{N\bar{L}} s_1^{iN} s_2^{jL}$$
$$+ \rho^{L\bar{T}} s_1^{iL} s_2^{jT} + \rho^{L\bar{N}} s_1^{iL} s_2^{jN} + \rho^{L\bar{L}} s_1^{iL} s_2^{jL})(\hat{\sigma}_i \otimes \hat{\sigma}_j)\Big). \qquad (10)$$

The relation between the un-normalized double-spin density matrix and the differential cross section is given by

$$d\sigma(\vec{s}_1, \vec{s}_2) = \frac{1}{2q^2}\rho(\vec{s}_1, \vec{s}_2)dPS. \qquad (11)$$

For a two-particle final state as in $e^+e^- \to t\bar{t}$ the Lorentz-invariant phase space dPS is given by

$$dPS_2 = \frac{v}{16\pi}d\cos\theta, \qquad (12)$$

where $v = \sqrt{1 - \xi}$, $\xi = 4m^2/q^2$, and θ is the polar angle between the momenta of the electron and the top quark. For the three-particle final state $t\bar{t}G$ one has two additional integration parameters $y := 1 - 2(p_1 q)/q^2$ and $z := 1 - 2(p_2 q)/q^2$ which are related to the energies $E_1 = p_1 q/\sqrt{q^2}$ and $E_2 = p_2 q/\sqrt{q^2}$ of the top quark and the antitop quark in the laboratory frame. In terms of the parameters y and z the three-particle phase space reads

$$dPS_3 = \frac{q^2}{32(2\pi)^4}dy\,dz\,d\cos\theta\,d\chi, \qquad (13)$$

where χ is the azimuthal angle between the beam plane spanned by the electron and the top quark, and the event plane spanned by the top quark and the antitop quark (or gluon).

B. Observables

We loosely refer to the single-spin polarization vectors and the spin-spin correlation tensors as observables even if the observability of these objects needs to be specified by e.g. their subsequent decay distributions. We shall return to this point in the next subsection.

Following Refs. [17,18] we define the observables

$$O^{e_1 e_2} = \frac{d\sigma^{e_1 e_2}}{d\sigma}, \qquad O^{e_1} = \frac{d\sigma^{e_1}}{d\sigma}, \qquad (14)$$

where $\vec{e}_1$ and $\vec{e}_2$ now are elements of the *same* frame, for which, as in Refs. [17,18], we choose the top quark rest frame. Differing from Refs. [17,18] we use an orthonormal basis in the top quark rest frame. As in Ref. [30] the three orthonormal basis vectors are defined by

$$\hat{t} = \frac{(\vec{p}_{e^-} \times \vec{p}_t) \times \vec{p}_t}{|(\vec{p}_{e^-} \times \vec{p}_t) \times \vec{p}_t|}, \qquad \hat{n} = \frac{\vec{p}_{e^-} \times \vec{p}_t}{|\vec{p}_{e^-} \times \vec{p}_t|}, \qquad \hat{l} = \frac{\vec{p}_t}{|\vec{p}_t|}. \qquad (15)$$

The three orthonormal basis vectors $(\hat{t}, \hat{n}, \hat{l})$ define our right-handed orthonormal frame. In order to check on the results of Refs. [17,18] we have also worked in the nonorthogonal frame $(\hat{k}, \hat{p}, \hat{n})$ employed in Ref. [17] where $\hat{k} = \hat{l}$ and $\hat{p} = \vec{p}_{e^-}/|\vec{p}_{e^-}|$. Our unit vector $\hat{t}$ can be seen to be a linear superposition of the unit vectors $\hat{k}$ and $\hat{p}$ given by

$$\hat{t} = \frac{\hat{k}\cos\theta - \hat{p}}{\sin\theta}. \qquad (16)$$

Returning to Eq. (14), the numerators in Eq. (14) are calculated according to

$$d\sigma^{e_1 e_2} = \frac{1}{2q^2}\mathrm{Tr}\left(\hat{\rho}e_1^i\frac{1}{2}\hat{\sigma}_i \otimes e_2^j\frac{1}{2}\hat{\sigma}_j\right)dPS = \frac{1}{2q^2}\rho^{e_1 e_2}dPS, \qquad (17)$$

$$d\sigma^{e_1} = \frac{1}{2q^2}\mathrm{Tr}\left(\hat{\rho}e_1^i\frac{1}{2}\hat{\sigma}_i \otimes \mathbb{1}\right)dPS = \frac{1}{2q^2}\rho^{e_1}dPS. \qquad (18)$$

The unpolarized rate in the denominators of Eq. (14) provides for the appropriate normalization and can be calculated according to

$$d\sigma = \frac{1}{2q^2}\mathrm{Tr}(\hat{\rho}\mathbb{1} \otimes \mathbb{1})dPS = \frac{1}{2q^2}\rho dPS. \qquad (19)$$

The phase space element dPS is rather symbolic and stands for a generic phase space element that remains after single or multiple phase space integrations. Summing up events in terms of polarization degrees according to the three quantization axes along $\hat{t}$, $\hat{n}$ and $\hat{l}$, one obtains contributions to a correlation matrix. This, however, is still not the quantity observed in the experiment. The polarization unveils itself rather by angular distributions of the subsequent decays of the top and antitop quarks.

C. Polarization analysis via subsequent cascade decays

In this subsection we discuss two measurements that allow one to analyze two particular linear combinations of the spin-spin coefficient functions. These measurements employ the inclusive semileptonic decays $t(\uparrow)/\bar{t}(\uparrow) \to \ell^+/\ell^- + X$ derived from the dominant decays $t \to b\ell^+\nu_\ell$ and $\bar{t} \to \bar{b}\ell^-\bar{\nu}_\ell$ and require the reconstruction of the momentum directions of the charged leptons in the respective top/antitop rest frames.

There are two ways to analyze the polarization of the top quark. The first is to treat the decay $t \to b + W^+(\to \ell^+ + \nu)$ as a cascade decay process [31–33]. The second way is to analyze the polarized top decay directly in the top quark rest frame [34]. We shall use the second possibility as has also been done in Ref. [26]. In our theoretical analysis we work in the narrow-width approximation for the top and antitop quarks which is well justified since the top quark width is much smaller than its mass. In order to describe the spin dependence of the cascade decays $e^+e^- \to t(\to b + \ell^+ + \nu_\ell) + \bar{t}(\to \bar{b} + \ell^- + \bar{\nu}_\ell)$ we employ the density matrix formalism of Ref. [26]. The whole cascade process is written in product form in terms of the production density matrix and the two decay density matrices. The absolute square of the matrix element for the cascade process

including the spin-density matrices $\hat{\rho}(t)$ and $\hat{\rho}(\bar{t})$ for the decay of the top and antitop quark, respectively, is proportional to the trace

$$\mathrm{Tr}(\hat{\rho}(t\bar{t})(\hat{\rho}(t) \otimes \hat{\rho}(\bar{t}))) = \hat{\rho}_{\lambda_1'\lambda_1}(t)\hat{\rho}_{\lambda_1\lambda_2,\lambda_1'\lambda_2'}(t\bar{t})\hat{\rho}_{\lambda_2'\lambda_2}(\bar{t}), \qquad (20)$$

where $\hat{\rho}(t\bar{t})$ is the double density matrix calculated in this paper.

The spin-density matrices for the two decaying top and antitop quarks are given by

$$\hat{\rho}(t) = \frac{\rho(t)}{2}(\mathbb{1} + \alpha(t)\hat{q}_1 \cdot \hat{\sigma}),$$

$$\hat{\rho}(\bar{t}) = \frac{\rho(\bar{t})}{2}(\mathbb{1} - \alpha(\bar{t})\hat{q}_2 \cdot \hat{\sigma}), \qquad (21)$$

where $\rho(t)$ and $\rho(\bar{t})$ are the partial widths of the corresponding decay channel for the decay of the polarized top and antitop quark, respectively, and $\alpha(t)$ and $\alpha(\bar{t})$ are the analyzing powers of the corresponding decay for the top and antitop spin, respectively, along the flight directions of the analyzing decay particles given by their three-momentum vector directions $\hat{q}_1$ and $\hat{q}_2$ in the rest frames of the top and antitop quark, respectively. If the decay channels are charge conjugate to each other as in our case for the top and antitop quark, the partial widths and the analyzing powers are equal, $\rho(\bar{t}) = \rho(t)$ and $\alpha(\bar{t}) = \alpha(t)$.

The analyzing power of the final state lepton has been analyzed in Refs. [35–37] including radiative corrections. The Born term analyzing powers of the three final-state particles in the decay ℓ^+, b and ν_ℓ have been summarized in Table 3 in Ref. [38]. The LO spin analyzing power in this decay was found to be 100% if one uses the momentum of the charged lepton as the analyzer. Because the decay $t(\uparrow) \to b\ell^+\nu_\ell$ has the same flavor structure, the result of Ref. [38] can be carried over to the present case. Let us define unit vectors $\hat{q}_i$ in the direction of the charged leptons ($i = 1$, 2 stand for ℓ^+, ℓ^-). These unit vectors can be expanded in the frame $(\hat{t}, \hat{n}, \hat{l})$ to obtain

$$\hat{q}_i = \hat{t}q_i^t + \hat{n}q_i^n + \hat{l}q_i^l$$
$$= \hat{t}\sin\theta_i\cos\chi_i + \hat{n}\sin\theta_i\sin\chi_i + \hat{l}\cos\theta_i, \qquad (22)$$

where θ_i is the polar angle and χ_i is the azimuthal angle of the respective charged lepton in the rest frames of the top and antitop quark. The calculation of the trace in Eq. (20) results in

$$\rho(t)^2\left(\rho + \sum_i \rho^{P_i}q_1^{P_i} - \sum_j \rho^{P_j}q_2^{P_j} - \sum_{i,j} \rho^{P_iP_j}q_1^{P_i}q_2^{P_j}\right). \qquad (23)$$

If only the polar angles θ_i are observed, the integration over the nonobserved azimuthal angles χ_i normalized by $(2\pi)^{-1}$ results in

$$\rho(t)^2 \rho(1 + \langle \mathcal{O}^l \rangle \cos\theta_1 - \langle \mathcal{O}^l \rangle \cos\theta_2 - \langle \mathcal{O}^{ll} \rangle \cos\theta_1 \cos\theta_2), \tag{24}$$

where $\langle \cdots \rangle$ denotes integration over the whole phase space. It is apparent that one can measure the observables $\langle \mathcal{O}^l \rangle$ and $\langle \mathcal{O}^{ll} \rangle$ by analyzing the polar angle dependence of the inclusive decays $t(\uparrow)/\bar{t}(\uparrow) \rightarrow \ell^+/\ell^- + X$. Other single-spin and spin-spin polarization observables can be measured by analyzing in addition the azimuthal angular dependence of the decays $t(\uparrow)/\bar{t}(\uparrow) \rightarrow \ell^+/\ell^- + X$.

The opening angle ϕ between the two charged leptons is defined by $\hat{q}_1 \cdot \hat{q}_2 = \cos\phi$. In order to determine the opening angle distribution one has to integrate over all angles except for ϕ, i.e. the azimuthal angle χ of an expansion of $\hat{q}_2$ in terms of $\hat{q}_1$ and two arbitrary perpendicular directions, and over all angles that determine the orientation of $\hat{q}_1$. The first normalized integration results in

$$\frac{1}{2\pi} \int \text{Tr}(\hat{\rho}(t\bar{t})(\hat{\rho}(t) \otimes \hat{\rho}(\bar{t}))) d\chi$$

$$= \frac{\rho(t)^2}{2\pi} \int \text{Tr}\left(\hat{\rho} \left(\frac{1}{2}(\mathbb{1} + \hat{q}_1 \cdot \hat{\sigma}) \otimes \frac{1}{2}(\mathbb{1} - \hat{q}_2 \cdot \hat{\sigma}) \right) \right) d\chi$$

$$= \frac{\rho(t)^2}{4} \{ \text{Tr}(\hat{\rho}) + \text{Tr}(\hat{\rho}(\hat{q}_1 \cdot \hat{\sigma} \otimes \mathbb{1}))$$

$$- [\text{Tr}(\hat{\rho}(\mathbb{1} \otimes \hat{q}_1 \cdot \hat{\sigma})) - \text{Tr}(\hat{\rho}(\hat{q}_1 \cdot \hat{\sigma} \otimes \hat{q}_1 \cdot \hat{\sigma}))] \cos\phi \}. \tag{25}$$

Expanding $\hat{q}_1 = \hat{t}\sin\theta_1 \cos\chi_1 + \hat{n}\sin\theta_1 \sin\chi_1 + \hat{l}\cos\theta_1$ as before, integrating over the solid angle with $d\chi_1 d(\cos\theta_1)$ and normalizing by $(4\pi)^{-1}$, one finally obtains

$$\frac{1}{8\pi^2} \int \text{Tr}(\hat{\rho}(t\bar{t})(\hat{\rho}(t) \otimes \hat{\rho}(\bar{t}))) d\chi d\chi_1 d(\cos\theta_1)$$

$$= \rho(t)^2 \rho \left(1 - \frac{1}{3}(\langle \mathcal{O}^{tt} \rangle + \langle \mathcal{O}^{nn} \rangle + \langle \mathcal{O}^{ll} \rangle) \cos\phi \right). \tag{26}$$

Therefore, the trace $\text{Tr}\mathcal{O} = \mathcal{O}^{tt} + \mathcal{O}^{nn} + \mathcal{O}^{ll}$ of the three-dimensional correlation matrix in phase-space integrated form can be determined by measuring the opening angle distribution. In Ref. [17] this observable was called $\mathcal{O}_4$. Note that because this observable is equally derived from the trace of $\hat{\rho}$ with the tensor product of the spin operator with itself, the value is equal to 1 at LO and decreases slightly if we include first-order radiative corrections. Therefore, the dependence on $\cos\phi$ is at most $1/3$ of the integrated contribution.

III. RESULTS UP TO $O(\alpha_s)$

Before presenting our NLO results derived from the one-loop and tree-graph contributions, we begin by presenting the Born term results. Equivalent results have already been listed in Ref. [17] where, however, a different representation has been used. The unpolarized Born term contribution is given by

$$\rho = e^4 N_c [(1 + v^2 \cos^2\theta) g_{11} + (1 - v^2) g_{12} + 2v \cos\theta g_{44}] \tag{27}$$

$(e^2 = 4\pi\alpha)$. Replacing $g_{11} = g_{PC}^{VV} + g_{PC}^{AA}$, $g_{12} = g_{PC}^{VV} - g_{PC}^{AA}$ and integrating over $\cos\theta$, this result is in agreement with the well-known result

$$\sigma = \frac{4\pi\alpha^2}{3q^2} N_c v \left(\frac{3 - v^2}{2} g_{PC}^{VV} + v^2 g_{PC}^{AA} \right). \tag{28}$$

The various single-spin and spin-spin contributions have been defined in Eqs. (17) and (18). They can be calculated using the leading-order form of Eq. (7). One has $(\xi = 1 - v^2)$

$$\rho^t = -e^4 N_c \sqrt{\xi} \sin\theta [v \cos\theta g_{14} + g_{41} + g_{42}],$$

$$\rho^n = -e^4 N_c \sqrt{\xi} v \sin\theta g_{43},$$

$$\rho^l = e^4 N_c [v(1 + \cos^2\theta) g_{14}$$
$$+ \cos\theta((1 + v^2) g_{41} + (1 - v^2) g_{42})],$$

$$\rho^{tt} = e^4 N_c \sin^2\theta (\xi g_{11} + g_{12}),$$

$$\rho^{tn} = \rho^{nt} = e^4 N_c v \sin^2\theta g_{13},$$

$$\rho^{tl} = \rho^{lt} = -e^4 N_c \sqrt{\xi} [\sin\theta \cos\theta (g_{11} + g_{12}) + v \sin\theta g_{44}],$$

$$\rho^{nn} = -e^4 N_c v^2 \sin^2\theta g_{12},$$

$$\rho^{nl} = \rho^{ln} = -e^4 N_c v \sqrt{\xi} \sin\theta \cos\theta g_{13},$$

$$\rho^{ll} = e^4 N_c [(v^2 + \cos^2\theta) g_{11} + \xi \cos^2\theta g_{12} + 2v \cos\theta g_{44}]. \tag{29}$$

Using Eq. (16), the LO coefficient functions listed in this subsection can be converted to the corresponding coefficient functions of Ref. [17].

A. $O(\alpha_s)$ loop contributions

The one-loop QCD vertex corrections have been calculated before in e.g. Refs. [8,12]. They can be expressed in terms of the two invariants A and B appearing in the covariant expansion of the matrix element $\langle t\bar{t}|j^\mu|0 \rangle$. They read

$$\mathrm{Re}A = -\frac{\alpha_s C_F}{4\pi v}\left[\left(\frac{1}{\varepsilon} - \gamma_E + \ln\left(\frac{4\pi\mu^2}{m^2}\right)\right)\left(2v - (1+v^2)\ln\left(\frac{1+v}{1-v}\right)\right)\right.$$
$$\left. + (1+v^2)\left(\mathrm{Li}_2\left(\frac{2v}{1+v}\right) - \mathrm{Li}_2\left(\frac{-2v}{1-v}\right) - \pi^2\right) - 3v^2\ln\left(\frac{1+v}{1-v}\right) + 4v\right],$$
$$\mathrm{Re}B = -\frac{\alpha_s C_F}{4\pi v}(1-v^2)\ln\left(\frac{1+v}{1-v}\right), \qquad \mathrm{Im}B = \frac{\alpha_s C_F}{4\pi v}(1-v^2)\pi, \tag{30}$$

where μ is the renormalization scale. The IR singularity is regularized by the parameter $\varepsilon = (4 - D)/2$ of dimensional regularization, $C_F = (N_c^2 - 1)/(2N_c) = 4/3$ for $N_c = 3$, and $\gamma_E = 0.577\ldots$ is the Euler-Mascheroni constant. The dimensional IR regularization parameter $1/\varepsilon$ can be converted to the gluon mass parameter used in the IR regularization of the tree graph integrations according to

$$\ln\Lambda \leftrightarrow \frac{1}{\varepsilon} - \gamma_E + \ln\left(\frac{4\pi\mu^2}{q^2}\right), \tag{31}$$

where $\Lambda = m_G^2/q^2$ is the normalized squared gluon mass. After folding the one-loop corrections with the Born term vertex function (spins not summed!) one obtains

$$\rho = e^4 N_c[(2(1 + v^2\cos^2\theta)\mathrm{Re}A - v^2(1 + 3\cos^2\theta)\mathrm{Re}B)g_{11} + (2\xi\mathrm{Re}A + v^2(3 + \cos^2\theta)\mathrm{Re}B)g_{12}$$
$$- 4v\cos\theta\mathrm{Im}Bg_{43} + 4v\cos\theta\mathrm{Re}(A - B)g_{44}],$$
$$\rho^{tt} = e^4 N_c\sin^2\theta[(2\xi\mathrm{Re}A + 3v^2\mathrm{Re}B)g_{11} + (2\mathrm{Re}A - v^2\mathrm{Re}B)g_{12}],$$
$$\rho^{tn} = \rho^{nt} = 2e^4 N_c v\sin^2\theta[(\mathrm{Re}A - \mathrm{Re}B)g_{13} + \mathrm{Im}Bg_{14}],$$
$$\rho^{tl} = \rho^{lt} = -\frac{e^4 N_c}{\sqrt{\xi}}[\sin\theta\cos\theta(2\xi\mathrm{Re}A + v^2\mathrm{Re}B)(g_{11} + g_{12}) - v(1 + \xi)\sin\theta\mathrm{Im}Bg_{43} + v\sin\theta(2\xi\mathrm{Re}A + (1 - 3\xi)\mathrm{Re}B)g_{44}],$$
$$\rho^{nn} = -e^4 N_c v^2\sin^2\theta[\mathrm{Re}Bg_{11} + (2\mathrm{Re}A - 3\mathrm{Re}B)g_{12}],$$
$$\rho^{nl} = \rho^{ln} = -e^4 N_c\frac{v}{\sqrt{\xi}}[\sin\theta\cos\theta(2\xi\mathrm{Re}A + (1 - 3\xi)\mathrm{Re}B)g_{13} + (1 + \xi)\sin\theta\cos\theta\mathrm{Im}Bg_{14} - v\sin\theta\mathrm{Im}B(g_{41} + g_{42})],$$
$$\rho^{ll} = e^4 N_c[(2(v^2 + \cos^2\theta)\mathrm{Re}A - v^2(3 + \cos^2\theta)\mathrm{Re}B)g_{11} + (2\xi\cos^2\theta\mathrm{Re}A + v^2(1 + 3\cos^2\theta)\mathrm{Re}B)g_{12}$$
$$- 4v\cos\theta\mathrm{Im}Bg_{43} + 4v\cos\theta(\mathrm{Re}A - \mathrm{Re}B)g_{44}]. \tag{32}$$

B. $O(\alpha_s)$ tree-graph contributions

According to the Lee-Nauenberg theorem, the IR singularities of the $O(\alpha_s)$ loop calculation are canceled against the IR singularities appearing in the tree graph calculation. In Ref. [39] we cut on the hard gluon phase space from above. In this paper we consider the full three-particle phase space. Let us specify the kinematics of the three-body decay more explicitly. We work in the laboratory frame with the z axis defined by the top quark momentum direction. The four-momenta q and p_1, p_2 read

$$q = \sqrt{q^2}(1; 0, 0, 0),$$
$$p_1 = \frac{1}{2}\sqrt{q^2}(1 - y; 0, 0, R_y),$$
$$p_2 = \frac{1}{2}\sqrt{q^2}(1 - z; R_z\sin\theta_{12}, 0, R_z\cos\theta_{12}) \tag{33}$$

where $R_y = \sqrt{(1 - y)^2 - \xi}$ and $R_z = \sqrt{(1 - z)^2 - \xi}$. The gluon momentum p_3 is given by $p_3 = q - p_1 - p_2$. The sine and the cosine of the polar angle θ_{12} between the momenta of the top and antitop quark are given by

$$\sin\theta_{12} = \frac{\sqrt{4yz(1 - y - z) - \xi(y + z)^2}}{R_y R_z},$$
$$\cos\theta_{12} = -\frac{1 - y - z - yz - \xi}{R_y R_z}. \tag{34}$$

The spin four-vectors satisfy $s_i p_i = 0$ and $s_i^2 = -1$. Including a sign for the orientation, they are given by

$$\pm s_1^L = \frac{\pm 1}{\sqrt{\xi}}(R_y; 0, 0, 1 - y),$$

$$\pm s_2^L = \frac{\pm 1}{\sqrt{\xi}}(R_z; (1 - z)\sin\theta_{12}, 0, (1 - z)\cos\theta_{12}),$$

$$\pm s_1^T = \pm(0; 1, 0, 0),$$

$$\pm s_2^T = \pm(0; \cos\theta_{12}, 0, -\sin\theta_{12}),$$

$$\pm s_1^N = \pm s_2^N = \pm(0; 0, 1, 0). \qquad (35)$$

Finally, the event plane spanned by the momenta of the top quark, antitop quark and gluon is rotated with respect to the beam plane which is spanned by the momenta of the electron and the top quark by an azimuthal angle χ. Viewed from the event plane the electron and positron have the four-momenta

$$p_\pm = \frac{1}{2}\sqrt{q^2}(1; \pm\cos\chi\sin\theta, \mp\sin\chi\sin\theta, \mp\cos\theta). \quad (36)$$

We do not list the explicit forms of the tree-graph contributions but merely catalog the generic structure of the integrals that appear in the phase space integration. The basic integrals have the structure

$$I_{n_y n_z}(m_y, m_z) = \int_{y_-}^{y_+} dy \int_{z_-(y)}^{z_+(y)} dz y^{m_y} z^{m_z} R_y^{n_y} R_z^{n_z}, \quad (37)$$

where n_y ranges from 0 to -4 and n_z takes the values 0 and -2. The indices m_y, m_z are limited from below by $m_y + m_z \geq -2$ and $m_y, m_z \geq -2$. The integrals with $m_y + m_z = -2$ are IR singular. For the regularization of the IR singularity at $y = z = 0$ we use a finite gluon mass $m_G = \sqrt{\Lambda q^2}$, such that the phase space limits are now given by $y_- = \Lambda + \sqrt{\Lambda\xi}$, $y_+ = 1 - \sqrt{\xi}$ and

$$z_\pm(y) = \frac{1}{4y + \xi}\Big(2y - 2y^2 - \xi y + 2\Lambda y + 2\Lambda$$
$$\pm 2R_y\sqrt{(y - \Lambda)^2 - \Lambda\xi}\Big). \qquad (38)$$

The subtraction of the singularity is performed by adding and subtracting an integral with the same singular behavior but with a simpler integrand. The simplified integrand is obtained from the original integrand by an expansion around $y = 0$. In this expansion, both R_y and R_z are replaced by v, leading to the generic divergent parts

$$I_D(-2, 0) = \frac{4v}{\xi}\int_{\Lambda+\sqrt{\Lambda\xi}}^{1-\sqrt{\xi}} \frac{dy}{y^2}\sqrt{(y - \Lambda)^2 - \Lambda\xi} = \frac{4v}{\xi}\left(\ln\left(\frac{2(1 - \sqrt{\xi})}{\sqrt{\Lambda\xi}}\right) - 1\right),$$

$$I_D(0, -2) = \int_{\Lambda+\sqrt{\Lambda\xi}}^{1-\sqrt{\xi}} dy\left(\frac{1}{z_-^s(y)} - \frac{1}{z_+^s(y)}\right) = \frac{4v}{\xi}\ln\left(\frac{2(1 - \sqrt{\xi})}{\sqrt{\Lambda\xi}}\right) - 2\frac{1 + v^2}{1 - v^2}\ln\left(\frac{1 + v}{1 - v}\right),$$

$$I_D(-1, -1) = \int_{\Lambda+\sqrt{\Lambda\xi}}^{1-\sqrt{\xi}} \frac{dy}{y}\ln\left(\frac{z_+^s(y)}{z_-^s(y)}\right) = I_D - \ln\left(\frac{1 + v}{1 - v}\right)\ln\Lambda, \qquad (39)$$

where $\xi z_\pm^s(y) = (1 + v^2)y \pm 2v\sqrt{(y - \Lambda)^2 - \Lambda\xi}$ and

$$I_D := 2\ln\left(\frac{1 - \sqrt{\xi}}{\sqrt{\xi}}\right)\ln\left(\frac{1 + v}{1 - v}\right) - \text{Li}_2\left(\frac{2v}{(1 + v)^2}\right) + \text{Li}_2\left(\frac{-2v}{(1 - v)^2}\right) + \frac{1}{2}\text{Li}_2\left(-\frac{(1 - v)^2}{(1 + v)^2}\right) - \frac{1}{2}\text{Li}_2\left(-\frac{(1 + v)^2}{(1 - v)^2}\right). \quad (40)$$

The results for the generic divergent parts in Eq. (39) are only accurate up to power-suppressed terms in $\sqrt{\Lambda}$. Adding and subtracting these divergent parts (including a corresponding factor $v^{n_y+n_z}$), the difference between the original integral and the divergent part turns out to be IR finite. This is equivalent to adding counterterms to the original unregularized integrals. The counterterms take the form

$$I_D(-2, 0), I_D(0, -2) \rightarrow \frac{4v}{\xi}\int_0^{1-\sqrt{\xi}} \frac{dy}{y},$$

$$I_D(-1, -1) \rightarrow 2\ln\left(\frac{1 + v}{1 - v}\right)\int_0^{1-\sqrt{\xi}} \frac{dy}{y}. \qquad (41)$$

After having removed the IR singularities it is not difficult to do the z-integration. One encounters integrals of the form

$$\int z^{-1} R_z^{-2} dz = \frac{\ln z}{1 - \xi} + \frac{\ln(1 - z + \sqrt{\xi})}{2(1 + \sqrt{\xi})\sqrt{\xi}} - \frac{\ln(1 - z - \sqrt{\xi})}{2(1 - \sqrt{\xi})\sqrt{\xi}}. \qquad (42)$$

In the subsequent y integration one encounters integrands of the form

$$L_0 = [\ln z]_{z_-(y)}^{z_+(y)}, \qquad L_\pm = [\ln (1 - z \pm \sqrt{\xi})]_{z_-(y)}^{z_+(y)}. \quad (43)$$

To do the y integration one uses the substitution

$$y = 1 - \frac{\sqrt{\xi}}{2}\left(t + \frac{1}{t}\right) \quad (44)$$

which allows one to factorize the arguments of the logarithms, e.g.

$$dy = -\frac{\sqrt{\xi}}{2}\left(1 - \frac{1}{t^2}\right)dt, \qquad R_y = \frac{\sqrt{\xi}}{2}\left(\frac{1}{t} - t\right),$$

$$L_0(t) = \ln\left(\frac{2 - \sqrt{\xi}t}{t(2t - \sqrt{\xi})}\right),$$

$$L_+(t) = 2\ln\left(\frac{(2 + \sqrt{\xi})t - \sqrt{\xi}}{2 + \sqrt{\xi} - \sqrt{\xi}t}\right) + \ln\left(\frac{2 - \sqrt{\xi}t}{t(2t - \sqrt{\xi})}\right),$$

$$L_-(t) = 2\ln\left(\frac{|(2 - \sqrt{\xi})t - \sqrt{\xi}|}{2 - \sqrt{\xi} - \sqrt{\xi}t}\right) + \ln\left(\frac{2 - \sqrt{\xi}t}{t(2t - \sqrt{\xi})}\right).$$

$$(45)$$

Note that for integrals containing L_- the substitution needs a subdivision of the integration interval $[t_-, t_1]$ into two parts, divided by the point t_0 where

$$t_\pm = \frac{1 \pm v}{\sqrt{\xi}}, \qquad t_0 = \frac{\sqrt{\xi}}{2 - \sqrt{\xi}}, \qquad t_+ t_- = 1. \quad (46)$$

It came as a surprise to us that in the end the contributions containing L_- in the integrand cancel (for a discussion, see Appendix A). One is finally left with three types of integrals

$$I_0^L(n) := \int L(t)t^{n-1}dt, \quad (47)$$

$$I_{1\pm}^L(n) := \int L(t)(1 \pm t)^{n-1}dt, \quad (48)$$

$$I_{t\pm}^L(n) := \int L(t)t_\pm^{-n}(t - t_\pm)^{n-1}dt, \quad (49)$$

where L stands for L_0, L_+ or can be skipped if no logarithm appears in the integrand. Our final results contain only those integrals (with $L = L_0, L_+$ and $n = 0$) which contain dilogarithms. All other contributions are at most logarithmic. These dilogarithmic integrals, together with the standard logarithmic integrals, are found in Appendix A.

C. $O(\alpha_s)$ total contributions

When one adds the $O(\alpha_s)$ loop and tree-graph contributions, one obtains IR-finite results. The list of results is quite long and they are presented in Appendix B. As an illustrative example we list the NLO unpolarized rate $\rho = g_{11}\rho_{11} + g_{12}\rho_{12} + g_{43}\rho_{43} + g_{44}\rho_{44}$ where the coefficients ρ_{ij} are given by

$$\rho_{11} = N\left[\frac{v}{4}((10 - \xi)(2 - 3\xi) - 3(4 - 20\xi + \xi^2)\cos^2\theta) + \frac{1}{8}(96 - 8\xi - 18\xi^2 + 3\xi^3 + (6 - \xi)(16 - 28\xi + 3\xi^2)\cos^2\theta)\ell_3 \right.$$

$$- \frac{1}{2}(8 - 2\xi + 3\xi^2 + (4 + \xi)(2 - 5\xi)\cos^2\theta)I_0^{L_0}(0) - \frac{\sqrt{\xi}}{2}(1 - \sqrt{\xi})(2 + 4\sqrt{\xi} - 3\xi)(1 - 3\cos^2\theta)I_{1-}^{L_0}(0)$$

$$- \frac{\sqrt{\xi}}{2}(1 + \sqrt{\xi})(2 - 4\sqrt{\xi} - 3\xi)(1 - 3\cos^2\theta)I_{1+}^{L_0}(0)$$

$$\left. + 2(1 + v^2\cos^2\theta)((1 + v^2)(\hat{I}_{t-}^{L_0}(0) + I_{t+}^{L_0}(0)) - 4v(\ell_0^- + \ell_0^+))\right], \quad (50)$$

$$\rho_{12} = N\xi\left[\frac{3v}{4}(14 - \xi - (6 - \xi)\cos^2\theta) + \frac{1}{8}(48 - 20\xi - 3\xi^2 + 3\xi(4 + \xi)\cos^2\theta)\ell_3 - \frac{1}{2}(8 - 5\xi + 3\xi\cos^2\theta)I_0^{L_0}(0) \right.$$

$$- \frac{\sqrt{\xi}}{2}(1 - \sqrt{\xi})(1 - 3\cos^2\theta)I_{1-}^{L_0}(0) - \frac{\sqrt{\xi}}{2}(1 + \sqrt{\xi})(1 - 3\cos^2\theta)I_{1+}^{L_0}(0)$$

$$\left. + 2((1 + v^2)(\hat{I}_{t-}^{L_0}(0) + I_{t+}^{L_0}(0)) - 4v(\ell_0^- + \ell_0^+))\right], \quad (51)$$

$$\rho_{43} = N\xi[-4\pi v \cos\theta], \quad (52)$$

$$\rho_{44} = N[-8\sqrt{\xi}(1 - \sqrt{\xi}) + 16\ell_2 + 4v(2 - 3\xi)\ell_3$$

$$- 2(4 - 5\xi)I_0^{L_0}(0) + 4v((1 + v^2)(\hat{I}_{t-}^{L_0}(0) - I_{t+}^{L_0}(0)) - 4v\ell_0^-)]\cos\theta. \quad (53)$$

The common factor N is given by

$$N = e^4 N_c \frac{\alpha_s C_F}{4\pi v} \qquad (54)$$

which is composed of the overall Born term factor $e^4 N_c$, the strong coupling factor α_s, the color factor C_F and the relative three-/two-particle phase space factor $(4\pi v)^{-1}$.

IV. NUMERICAL RESULTS AND COMPARISON

In order to check on our analytical results we compare them with the numerical results of Refs. [17,18]. Using the same values for the parameters as given in Refs. [17,18], we reproduce the entries of Table I in Ref. [17] with an accuracy of 0.2%. We also agree on the various figures presented in Ref. [18]. We remind the reader that we employ an orthonormal frame $(\hat{t}, \hat{n}, \hat{l})$ instead of the non-orthogonal frame $(\hat{k}, \hat{p}, \hat{n})$ of Ref. [17] and the un-normalized but orthogonal frame $(\hat{k}, \hat{k}^\perp, \hat{n})$ of Ref. [18].

A. Polar angle dependence for different energies

In Figs. 1–6 we present our results for some of the observables defined in Eq. (14). The full set of nine observables for the correlation matrix can be divided up into the diagonal elements $\mathcal{O}^{tt}$, $\mathcal{O}^{nn}$ and $\mathcal{O}^{ll}$, and a set of six off-diagonal elements. For the parameters we use the values [40]

$$m_Z = 91.1876(21) \text{ GeV}, \quad \Gamma_Z = 2.4952(23) \text{ GeV},$$
$$m_t = 174.6(1.9) \text{ GeV}$$
$$\sin^2\theta_W = 0.23126(5), \qquad \alpha_S(m_Z) = 0.1185(6),$$
$$G_F/(\hbar c)^3 = 1.1663787(6) \times 10^{-5} \text{ GeV}^{-2}. \qquad (55)$$

In Fig. 1 we plot the polar angle dependence of the dominant diagonal element $\mathcal{O}^{ll}$. The value is close to 100% in the forward and backward directions and decreases slightly with increasing center-of-mass energy $\sqrt{q^2}$. In
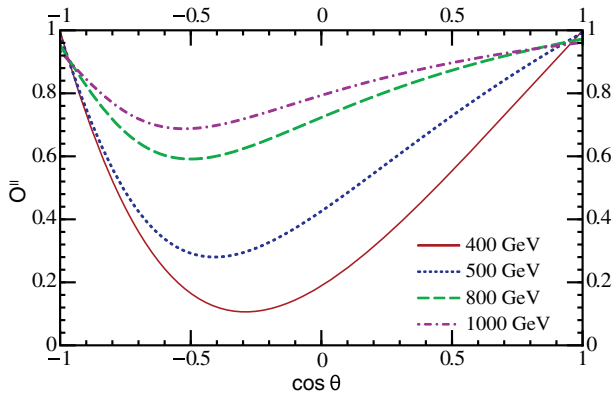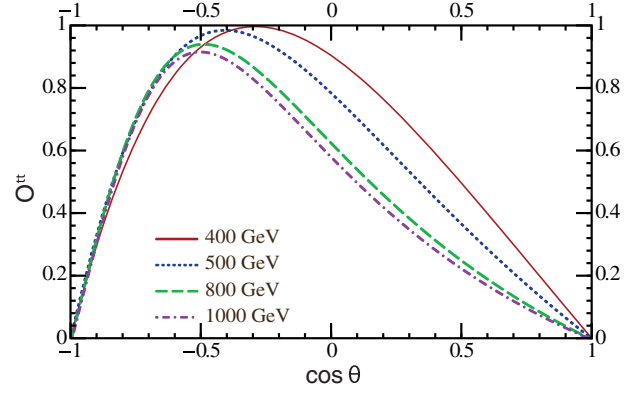

FIG. 2. The observable $\mathcal{O}^{tt}$ as a function of $\cos\theta$ for different energies $\sqrt{q^2} = 400$ (solid line), 500 (dotted), 800 (dashed), and 1000 GeV (dashed dotted).

the transverse direction the value falls off to 10% for $\sqrt{q^2} = 400$ GeV and only to 70% for $\sqrt{q^2} = 1000$ GeV while the location of the minimum tends to the backward direction.

While the depth of the minimum for $\mathcal{O}^{ll}$ decreases with increasing c.m. energy $\sqrt{q^2}$, the situation is reversed for $\mathcal{O}^{tt}$ shown in Fig. 2. In the forward and backward directions the value is exactly zero, as there is no boost that can turn the transversal direction into the direction of the quark, while the maximal value slightly falls from nearly 100% for $\sqrt{q^2} = 400$ GeV to 90% for $\sqrt{q^2} = 1000$ GeV. The position of the maximum of $\mathcal{O}^{tt}$ roughly coincides with the position of the minimum of $\mathcal{O}^{ll}$.

The remaining diagonal element $\mathcal{O}^{nn}$ is again exactly zero in the forward and backward directions. As shown in Fig. 3, the maximum of the absolute value of this (negative) observable $\mathcal{O}^{nn}$ increases from 10% for $\sqrt{q^2} = 400$ GeV to 70% for $\sqrt{q^2} = 1000$ GeV, with nearly the same position of the extremum as for $\mathcal{O}^{ll}$ and $\mathcal{O}^{tt}$.

FIG. 1. The observable $\mathcal{O}^{ll}$ as a function of $\cos\theta$ for different energies $\sqrt{q^2} = 400$ (solid line), 500 (dotted), 800 (dashed), and 1000 GeV (dashed dotted).
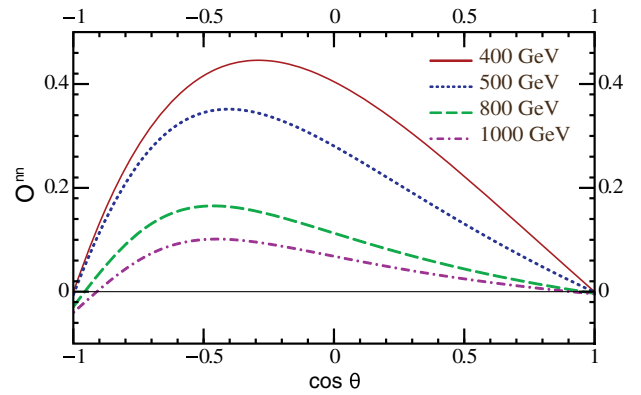

FIG. 3. The observable $\mathcal{O}^{nn}$ as a function of $\cos\theta$ for different energies $\sqrt{q^2} = 400$ (solid line), 500 (dotted), 800 (dashed), and 1000 GeV (dashed dotted).
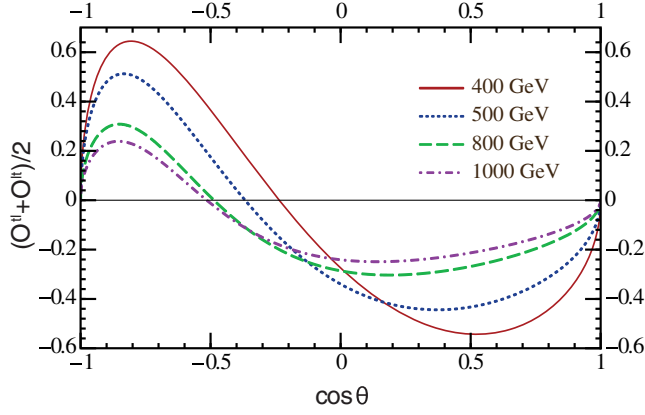
FIG. 4. $(\mathcal{O}^{tl} + \mathcal{O}^{lt})/2$ as a function of $\cos\theta$ for different energies $\sqrt{q^2} = 400$ (solid line), 500 (dotted), 800 (dashed), and 1000 GeV (dashed dotted).

FIG. 6. Trace $\mathrm{Tr}\mathcal{O}$ as a function of $\cos\theta$ for different energies $\sqrt{q^2} = 400$ (solid line), 500 (dotted), 800 (dashed), and 1000 GeV (dashed dotted).

Looking at the off-diagonal elements, the values for the observables $\mathcal{O}^{tl}$ and $\mathcal{O}^{lt}$ are very close, albeit not equal. In Fig. 4 the mean value $(\mathcal{O}^{tl} + \mathcal{O}^{lt})/2$ of these two observables is displayed. The value again vanishes in the forward and backward direction. The sine-type run of the curve for low energies is again shifted to the backward direction for higher energies while the absolute values are falling. The position of the zero crossing coincides again roughly with the positions of the extrema in the previous diagrams.

In Fig. 5 we show the normalized difference of the two adjoint nondiagonal elements, $(\mathcal{O}^{tl} - \mathcal{O}^{lt})/2$. Obviously, the normalized difference vanishes for small energies and increases to a maximum value of 2.3% for $\sqrt{q^2} = 1000$ GeV. However, for increasing energies the position of the maximum stays at a nearly constant value of approximately $\cos\theta = -0.67$.

In Fig. 6 the angular dependence of the trace $\mathrm{Tr}\mathcal{O} = \mathcal{O}^{tt} + \mathcal{O}^{nn} + \mathcal{O}^{ll}$ of the three-dimensional correlation matrix relevant for the opening angle distribution is shown. At threshold (and also at LO) the trace is 1 while for higher
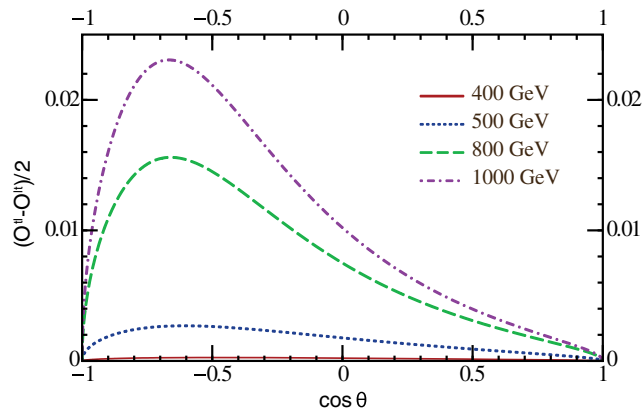

FIG. 5. $(\mathcal{O}^{tl} - \mathcal{O}^{lt})/2$ as a function of $\cos\theta$ for different energies $\sqrt{q^2} = 400$ (solid line), 500 (dotted), 800 (dashed), and 1000 GeV (dashed dotted).
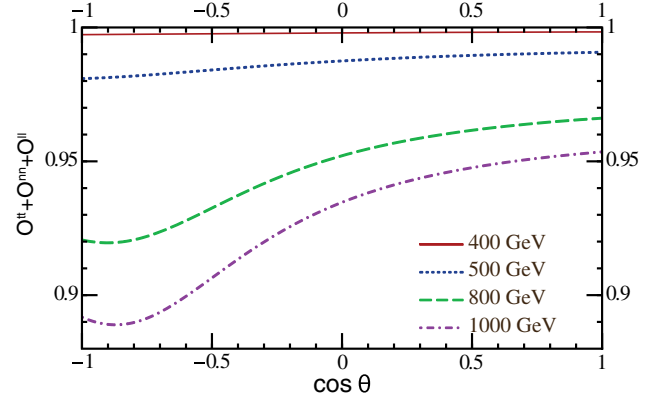
energies the value decreases especially in the backward direction.

B. Dependence on initial beam polarization

The initial beam polarization can be easily implemented by changing the electroweak coupling factors g_{ij} according to

$$g_{1j} \rightarrow (1 - h_- h_+)g_{1j} + (h_- - h_+)g_{4j},$$
$$g_{4j} \rightarrow (h_- - h_+)g_{1j} + (1 - h_- h_+)g_{4j}, \qquad (56)$$

where h_- and h_+ are twice the helicities of the initial electron and positron beams, respectively [30]. For the normalized density matrix elements one remains with the single parameter dependence given by Ref. [30]

$$P_{\mathrm{eff}} = \frac{h_- - h_+}{1 - h_- h_+}. \qquad (57)$$

It is clear that the two limiting cases $P_{\mathrm{eff}} = \pm 1$ cannot be realized technically. However, since the polarization effects are governed by P_{eff} and *not* by $h_\mp = -h_\pm = \mp 1$, one can get very close to the limiting cases $P_{\mathrm{eff}} = \mp 1$ with presently achievable degrees of beam polarization of $\sim 80\%$ (see the discussion in Ref. [30]). For example, for $h_- = -h_+ = -0.8$ one has $P_{\mathrm{eff}} = -0.976$. In Fig. 7 we show the dependence of $\mathcal{O}^{ll}$ on the polar angle for $\sqrt{q^2} = 1000$ GeV and the values $P_{\mathrm{eff}} = 0, \pm 1$. The dependence of the spin-spin correlation on the initial beam polarization turns out to be much smaller than the dependence of the single-spin polarization (cf. Ref. [30]). For $\mathcal{O}^{ll}$ it amounts to 10% close to $\cos\theta = -0.7$ while the single-spin observable can change locally by more than 100%.

C. Comparison with other publications

As mentioned earlier, we have checked that the single-spin observables are analytically identical to the one presented in Refs. [11–13]. This by-product in the present investigation provides a profound cross-check for our
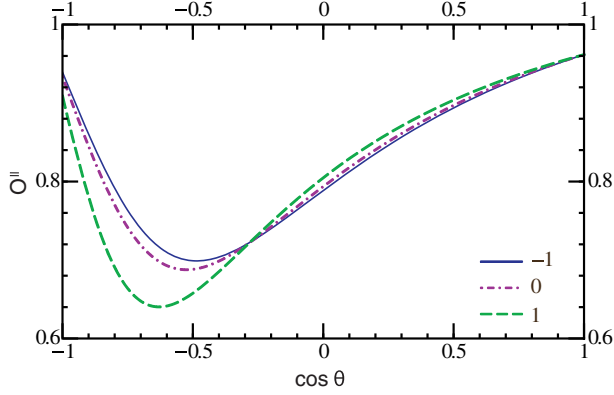
FIG. 7. The observable $\mathcal{O}^{ll}$ as a function of $\cos\theta$ for $\sqrt{q^2} = 1000$ GeV and different initial beam polarizations, given by $P_{\text{eff}} = 0, \pm 1$.

calculation. Because of the use of different observables, the results of Refs. [14–16] cannot be directly compared with $\mathcal{O}^{ll}$.[3] On the other hand, we obtain good agreement with the diagrams presented in Ref. [18].

V. RESULTS IN THE BASES OF PARKE AND SHADMI

Parke and Shadmi have discussed the case of completely polarized beams which leads to very simple rate and polarization formulas [19]. They considered the two cases LR ($h_- = -1$, $h_+ = 1$) and RL ($h_- = 1$, $h_+ = -1$). Here we concentrate on the case LR. Parke and Shadmi have introduced the chiral electroweak coupling factors f_{LL} and f_{LR} which can be related to our coupling factors g_{ij} by [30]

$$
\begin{aligned}
f_{LL} &= \sqrt{g_{11} - g_{14} - g_{41} + g_{44}} \\
&= Q_e Q_f + |\chi_Z|(v_e + a_e)(v_f + a_f), \\
f_{LR} &= \sqrt{g_{11} + g_{14} - g_{41} - g_{44}} \\
&= Q_e Q_f + |\chi_Z|(v_e + a_e)(v_f - a_f).
\end{aligned}
\tag{58}
$$

Since the production threshold for top quarks of mass 175 GeV is far above the Z boson pole, we neglect the Z width and we have therefore dropped the contributions of the coupling factors $g_{13,23}$, $g_{31,32}$ and $g_{34,43}$. For the case LR one has the following replacements:

$$
\begin{aligned}
g_{11} &\to 2g_{11} - 2g_{41} = f_{LL}^2 + f_{LR}^2, \\
g_{12} &\to 2g_{12} - 2g_{42} = 2f_{LL}f_{LR}, \\
g_{14} &\to 2g_{14} - 2g_{44} = -(f_{LL}^2 - f_{LR}^2), \\
g_{41} &\to 2g_{41} - 2g_{11} = -(f_{LL}^2 + f_{LR}^2), \\
g_{42} &\to 2g_{42} - 2g_{12} = -2f_{LL}f_{LR}, \\
g_{44} &\to 2g_{44} - 2g_{14} = f_{LL}^2 - f_{LR}^2.
\end{aligned}
\tag{59}
$$

---

[3]In Refs. [14–16], ρ^{LL} has been investigated.

For some frequently occurring linear combinations one obtains

$$
\begin{aligned}
g_{11} + g_{12} &\to +(f_{LL} + f_{LR})^2, \\
g_{11} - g_{12} &\to +(f_{LL} - f_{LR})^2, \\
g_{41} + g_{42} &\to -(f_{LL} + f_{LR})^2, \\
g_{41} - g_{42} &\to -(f_{LL} - f_{LR})^2.
\end{aligned}
\tag{60}
$$

Using the abbreviations ($v = \sqrt{1 - 4m^2/q^2}$)

$$
\begin{aligned}
A_{LR} &= f_{LL}(1 + v\cos\theta) + f_{LR}(1 - v\cos\theta), \\
T &= \sin\theta\sqrt{1 - v^2}(f_{LL} + f_{LR}), \\
L &= f_{LL}(\cos\theta + v) + f_{LR}(\cos\theta - v),
\end{aligned}
\tag{61}
$$

where $A_{LR}^2 = T^2 + L^2 + 4f_{LL}f_{LR}v^2\sin^2\theta$ and

$$
(1 \pm \cos\theta)^2(f_{LL}(1 \pm v) + f_{LR}(1 \mp v))^2 = (A_{RL} \pm L)^2,
\tag{62}
$$

we shall present our Born term results on the single- and double-spin density matrices in two different coordinate systems. These are the helicity basis and the off-diagonal basis introduced in Ref. [19].

A. Helicity basis

Rewriting the Born term results of Sec. III in terms of the chiral coupling factors f_{LL} and f_{LR}, the nonvanishing contributions are given by

$$
\begin{aligned}
\rho &= +e^4 N_c(T^2 + L^2 + 2f_{LL}f_{LR}v^2\sin^2\theta), \\
\rho^t &= +e^4 N_c T A_{LR}, \\
\rho^l &= -e^4 N_c L A_{LR}, \\
\rho^{tt} &= +e^4 N_c(T^2 + 2f_{LL}f_{LR}v^2\sin^2\theta), \\
\rho^{tl} &= \rho^{lt} = -e^4 N_c L T, \\
\rho^{nn} &= -2e^4 N_c v^2\sin^2\theta f_{LL}f_{LR}, \\
\rho^{ll} &= +e^4 N_c(L^2 + 2f_{LL}f_{LR}v^2\sin^2\theta).
\end{aligned}
\tag{63}
$$

From the single-spin density matrix elements ρ^t and ρ^l one can calculate the angle between the polarization vector of the top quark and the direction of the top quark. For definiteness we call this angle θ_{LR}. One has

$$
\frac{\sin\theta_{LR}}{\cos\theta_{LR}} = \frac{\rho^t}{\rho^l} = -\frac{TA_{LR}}{LA_{LR}} = -\frac{T}{L}.
\tag{64}
$$

We shall see that the direction of the polarization vector of the top quark defines the z direction of the off-diagonal basis of Parke and Shadmi.

In order to check on our results we calculate the rates $\rho(\uparrow,\uparrow)$, $\rho(\uparrow,\downarrow)$, $\rho(\downarrow,\uparrow)$ and $\rho(\downarrow,\downarrow)$. Note that Parke and Shadmi have defined the quantization axes as the momentum axes of the top and antitop quark, respectively. Therefore, the second arrow has to be reinterpreted to fit with our convention. Using both conventions, at the Born term level one obtains

$$\rho(t_\uparrow \bar{t}_\uparrow) = \rho(\uparrow,\downarrow) = \frac{1}{4}(\rho + \rho^{l_1} - \rho^{l_2} - \rho^{l_1 l_2})$$

$$= \frac{1}{4}(\rho - \rho^{ll}) = \frac{1}{4} e^4 N_c T^2, \qquad (65)$$

and $\rho(t_\downarrow \bar{t}_\downarrow) = \rho(\downarrow,\uparrow) = \rho(\uparrow,\downarrow) = \rho(t_\uparrow \bar{t}_\uparrow)$ since $\rho^{\ell_1} = \rho^{\ell_2} = \rho^l$. Furthermore, one obtains

$$\rho(t_\uparrow \bar{t}_\downarrow) = \rho(\uparrow,\uparrow) = \frac{1}{4}(\rho + \rho^{l_1} + \rho^{l_2} + \rho^{l_1 l_2}) = \frac{1}{4}(\rho + 2\rho^l + \rho^{ll})$$

$$= \frac{1}{4} e^4 N_c ((1 - \cos\theta)^2 (f_{LL}(1 - v) + f_{LR}(1 + v))^2),$$

$$\rho(t_\downarrow \bar{t}_\uparrow) = \rho(\downarrow,\downarrow) = \frac{1}{4}(\rho - \rho^{l_1} - \rho^{l_2} + \rho^{l_1 l_2}) = \frac{1}{4}(\rho - 2\rho^l + \rho^{ll})$$

$$= \frac{1}{4} e^4 N_c ((1 + \cos\theta)^2 (f_{LL}(1 + v) + f_{LR}(1 - v))^2) \qquad (66)$$

where we have used the relation (62). All rates agree with the results of Parke and Shadmi.

B. Off-diagonal basis

Parke and Shadmi have introduced an off-diagonal basis by demanding that the rates $\rho(t_\uparrow \bar{t}_\uparrow)$ and $\rho(t_\downarrow \bar{t}_\downarrow)$ vanish in that basis. We show that this demand leads to the condition that the angle θ_{LR} between the helicity basis and the off-diagonal basis is determined by Eq. (64). Let us consider the rate $\rho(t_\uparrow \bar{t}_\uparrow)'$ in the off-diagonal basis[4]

$$\vec{e}^{l'} = \cos\theta_{LR} \vec{e}^{l} + \sin\theta_{LR} \vec{e}^{t},$$
$$\vec{e}^{t'} = -\sin\theta_{LR} \vec{e}^{l} + \cos\theta_{LR} \vec{e}^{t}. \qquad (67)$$

Using the spin projection formula (17) and Eq. (65), at the Born term level one has

$$\rho(t_\uparrow \bar{t}_\uparrow)' = \frac{1}{4}(\rho - \cos^2\theta_{LR}\rho^{ll} - \sin^2\theta_{LR}\rho^{tt}$$

$$- 2\sin\theta_{LR}\cos\theta_{LR}\rho^{lt})$$

$$= \frac{1}{4} e^4 N_c (L\sin\theta_{LR} + T\cos\theta_{LR})^2. \qquad (68)$$

Therefore, the condition $\rho(t_\uparrow \bar{t}_\uparrow)' = 0$ defines the off-diagonal basis via the condition $L\sin\theta_{LR} + T\cos\theta_{LR} = 0$.

C. $O(\alpha_s)$ corrections

Parke and Shadmi [19] expressed their expectations that radiative corrections to their analysis of spin-spin correlations in $e^+ e^-$ annihilations are small. An attempt to estimate the effects of radiative corrections were published in Ref. [20]. However, since the calculation of Ref. [20] employed the soft-gluon approximation, the results are incomplete in the sense that spin-spin correlation effects due to hard gluon emission are missed in such a calculation. The present paper rectifies this omission.

Going beyond the Born term level, the simultaneous disappearance of $\rho^{t'}$ and $\rho(t_\uparrow \bar{t}_\uparrow)'$ is no longer granted. In this case one has to decide which of the two quantities is used to define the angle θ_{LR}. Here we decide to define the angle via the single-spin quantity, as it was done in Ref. [30]. This definition is physically more transparent. Furthermore it is also valid for unpolarized or partly polarized beams. In addition to the polar angle θ_{LR}, an azimuthal angle χ_{LR} has to be defined which points out of the plane spanned by the electron and top quark momenta. Actually, this azimuthal angle is already present at the Born term level if one takes into account the coupling factors g_{13} and g_{43}. The angles can be unambiguously defined by

$$\sin\theta_{LR} = \frac{\rho^t}{\sqrt{(\rho^t)^2 + (\rho^l)^2}}, \qquad \cos\theta_{LR} = \frac{\rho^l}{\sqrt{(\rho^t)^2 + (\rho^l)^2}} \qquad (69)$$

and

$$\sin\chi_{LR} = \frac{\rho^n}{\sqrt{(\rho^t)^2 + (\rho^n)^2 + (\rho^l)^2}},$$

$$\cos\chi_{LR} = \frac{\sqrt{(\rho^t)^2 + (\rho^l)^2}}{\sqrt{(\rho^t)^2 + (\rho^n)^2 + (\rho^l)^2}}. \qquad (70)$$

In Fig. 8 we show $\cos\theta_{LR}$ as a function of $\cos\theta$ for the four center-of-mass energies used throughout this paper.

---

[4]Note that the direction of the active angle θ_{LR} is opposed to the direction of the passive angle θ.
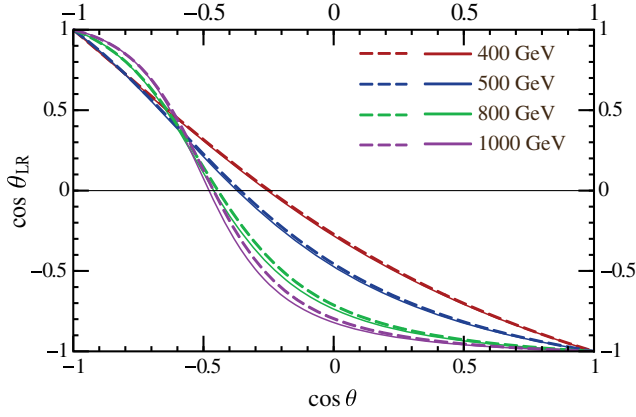
FIG. 8. $\cos\theta_{LR}$ as a function of $\cos\theta$ for different energies $\sqrt{q^2} = 400$ (red lines), 500 (blue), 800 (green), and 1000 GeV (purple), at $\cos\theta = 0$ distinguishable from top to bottom. While the color convention is the same as in Figs. 1–6, the line style distinguishes between Born term results (dashed lines) and $O(\alpha_s)$ results (solid lines).

The Born term result for $\sqrt{q^2} = 400$ GeV coincides perfectly with the result shown in Fig. 2 of Ref. [19], if we take into account that $\xi = -\theta_{LR}$ is defined counterclockwise. Radiative corrections vanish at the boundaries $\cos\theta = \pm 1$ and are maximal close to $\cos\theta = -0.2$ amounting to absolute changes of -1.0% ($\sqrt{q^2} = 400$ GeV), -1.9% (500 GeV), -3.8% (800 GeV), and -4.4% (1000 GeV).

While the irrelevance of the Z width far from the Z pole is nicely demonstrated by the fact that the absolute value of the azimuthal angle χ_{LR} at the Born term level is below 0.00035, due to the three-body kinematics of the final state the value for the azimuthal angle is 2 orders of magnitude higher if one includes $O(\alpha_s)$ radiative corrections. Note that χ_{LR} is an odd function of θ. Therefore, in Fig. 9 χ_{LR} is shown again as a function of $\cos\theta$ only.
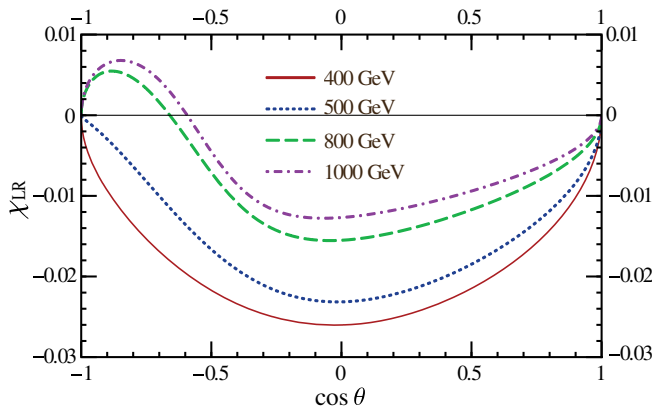

FIG. 9. χ_{LR} as a function of $\cos\theta$ for different energies $\sqrt{q^2} = 400$ (solid line), 500 (dotted), 800 (dashed), and 1000 GeV (dashed dotted). Born term results are 2 orders of magnitude smaller and coincide with the abscissa.
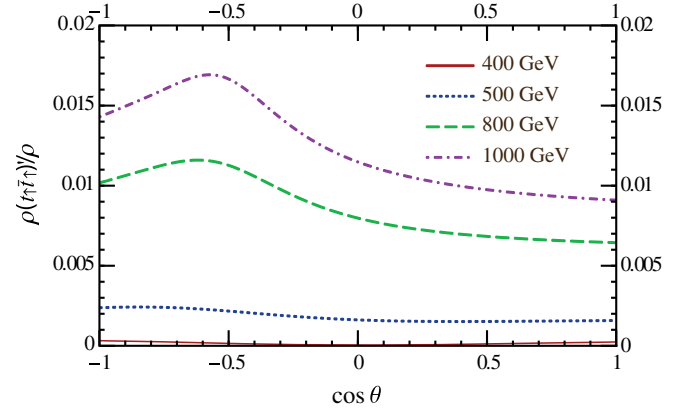

FIG. 10. $\rho(t_\uparrow\bar{t}_\uparrow)'/\rho$ as a function of $\cos\theta$ for different energies $\sqrt{q^2} = 400$ (solid line), 500 (dotted), 800 (dashed), and 1000 GeV (dashed dotted).

With θ_{LR} and χ_{LR} at hand, one finally can calculate the value for $\rho(t_\uparrow\bar{t}_\uparrow)'$. While this value is zero at the Born term level, with

$$\vec{e}^{\,l'} = \sin\theta_{LR}(\cos\chi_{LR}\vec{e}^{\,t} + \sin\chi_{LR}\vec{e}^{\,n}) + \cos\theta_{LR}\vec{e}^{\,l} \quad (71)$$

and using Eqs. (65) and (17) one obtains

$$
\begin{aligned}
\rho(t_\uparrow\bar{t}_\uparrow)' = \frac{1}{4}(&\rho - \rho^{tt}\sin^2\theta_{LR}\cos^2\chi_{LR} \\
&- \rho^{nn}\sin^2\theta_{LR}\sin^2\chi_{LR} - \rho^{ll}\cos^2\theta_{LR} \\
&- 2\rho^{tn}\sin^2\theta_{LR}\sin\chi_{LR}\cos\chi_{LR} \\
&- 2\rho^{tk}\sin\theta_{LR}\cos\theta_{LR}\cos\chi_{LR} \\
&- 2\rho^{nk}\sin\theta_{LR}\cos\theta_{LR}\sin\chi_{LR}).
\end{aligned} \quad (72)
$$

The result for the normalized quantity $\rho(t_\uparrow\bar{t}_\uparrow)'/\rho$ is shown in Fig. 10. For $\sqrt{q^2} = 400$ GeV the result is still very small with a minimum value of 0.005% close to $\cos\theta = 0$. The deviation grows for higher center-of-mass energies, and a maximum is found again close to $\cos\theta = -0.67$ with values of $\rho(t_\uparrow\bar{t}_\uparrow)'/\rho = 1.2\%$ and 1.7% for $\sqrt{q^2} = 800$ and 1000 GeV, respectively. This observation again confirms the rigidity of the back-to-back direction [21].

VI. SUMMARY AND CONCLUSION

We have presented the results of an analytical $O(\alpha_s)$ calculation of polarized top-antitop quark production in e^+e^- annihilation within the Standard Model. We have checked our results against previously available analytical $O(\alpha_s)$ results on single-spin polarization effects as well as previous numerical $O(\alpha_s)$ results on spin-spin polarization effects which were obtained with the phase space slicing method. Our results were presented in the

form of spin-spin density matrices defined in the respective rest frames of the top quark and antitop quark. Based on the spin-spin density formalism we discussed how the spin-spin correlations can be measured through an angular analysis of the polarized top quark decays $t(\uparrow) \to bW^+(\to \ell^+ + \nu)$ and the corresponding antitop quark decay. We have briefly discussed how to generalize our results to the case of polarized e^+e^- annihilation which has allowed us to discuss the $O(\alpha_s)$ corrections to the LO maximal spin-spin correlation effects in the off-diagonal basis which were discovered by Parke and Shadmi [19].

Our results have been obtained in the so-called beam frame defined by the incoming beam electron and the outgoing top quark. Corresponding $O(\alpha_s)$ results for the so-called event frame spanned by the top-antitop quark and the gluon will be presented in a forthcoming publication [23].

APPENDIX A: DILOGARITHMIC INTEGRALS

This appendix contains the standard logarithms and the dilogarithmic integrals which are the main building blocks for the $O(\alpha_s)$ final results. The logarithms necessary to write up the results are given by

$$\ell_0^- = \ln\left(\frac{4(1-\sqrt{\xi})}{\xi}\right), \qquad \ell_0^+ = \ln\left(\frac{2(1+\sqrt{\xi})}{\sqrt{\xi}}\right),$$

$$\ell_1 = \ln\left(\frac{\sqrt{\xi}(1+\sqrt{\xi})}{2}\right), \qquad \ell_2 = \ln\left(\frac{2-\sqrt{\xi}}{\sqrt{\xi}}\right), \qquad \ell_3 = \ln\left(\frac{1+v}{1-v}\right). \tag{A1}$$

The dilogarithmic integrals are given by Eq. (47) for $n = 0$. A special treatment is necessary for the integral $I_{t-}^{L_0}(0)$ because this integral is IR divergent. After extracting the divergent part according to the method explained in the main text, one is left with the subtracted integral

$$I_{t-}^{\prime L_0}(0) = \int_{t_-}^{t_1} \frac{L_0(t)dt}{t-t_-} - 2\ln\left(\frac{1+v}{1-v}\right) \int_{t_-}^{t_1} \left(\frac{dt}{t-t_-} + \frac{dt}{t-t_+} - \frac{dt}{t}\right)$$

$$= -\ln\left(\frac{1-v}{2(1+\sqrt{\xi})}\right)\ln\left(\frac{1+v}{1-v}\right) - \text{Li}_2\left(-\frac{1-v-\sqrt{\xi}}{1+v}\right) + \text{Li}_2\left(\frac{1-v-\sqrt{\xi}}{1-v}\right) + \text{Li}_2\left(2\frac{1-v-\sqrt{\xi}}{(1-v)^2}\right). \tag{A2}$$

As the IR divergence is general, the coefficient for this integral is also proportional to the Born term result. As such, one can resum the contributions from the IR-divergent part of the tree-term diagrams,

$$I_D = 2\ln\left(\frac{1-\sqrt{\xi}}{\sqrt{\xi}}\right)\ln\left(\frac{1+v}{1-v}\right) - \text{Li}_2\left(\frac{2v}{(1+v)^2}\right) + \text{Li}_2\left(\frac{-2v}{(1-v)^2}\right)$$

$$+ \frac{1}{2}\text{Li}_2\left(-\frac{(1-v)^2}{(1+v)^2}\right) - \frac{1}{2}\text{Li}_2\left(-\frac{(1+v)^2}{(1-v)^2}\right) \tag{A3}$$

and the contributions from the IR-divergent part of the one-loop diagrams,

$$I_L = \ln\left(\frac{\xi}{4}\right)\ln\left(\frac{1+v}{1-v}\right) + \text{Li}_2\left(\frac{2v}{1+v}\right) - \text{Li}_2\left(\frac{-2v}{1-v}\right) - \pi^2 \tag{A4}$$

to obtain

$$\hat{I}_{t-}^{L_0}(0) = I_{t-}^{\prime L_0}(0) + I_D - I_L. \tag{A5}$$

For the other dilogarithmic integrals there is no need for regularization. Using the known identities for dilogarithms, one can of course try hard to simplify the expressions in terms of dilogarithms and double logarithms. However, the outcome is still arbitrary and in general will not justify the effort. Still, we brought the results into a form which is manifestly real, obtaining

$$I_{t+}^{L_0}(0) = \ln\left(\frac{2(1+\sqrt{\xi})}{1+v}\right)\ln\left(\frac{1+v}{1-v}\right) + \mathrm{Li}_2\left(\frac{-2v}{1-v}\right) - \mathrm{Li}_2\left(\frac{2v}{1+v}\right) - \mathrm{Li}_2\left(\frac{4v}{(1+v)^2}\right)$$
$$- \mathrm{Li}_2\left(-\frac{1+v-\sqrt{\xi}}{1-v}\right) + \mathrm{Li}_2\left(\frac{1+v-\sqrt{\xi}}{1+v}\right) + \mathrm{Li}_2\left(2\frac{1+v-\sqrt{\xi}}{(1+v)^2}\right),$$

$$I_{1-}^{L_0}(0) = -\mathrm{Li}_2\left(\frac{1-v-\sqrt{\xi}}{2-\sqrt{\xi}}\right) + \mathrm{Li}_2\left(-\frac{1-v-\sqrt{\xi}}{\sqrt{\xi}}\right) + \mathrm{Li}_2\left(-2\frac{1-v-\sqrt{\xi}}{\sqrt{\xi}(2-\sqrt{\xi})}\right),$$

$$I_{1+}^{L_0}(0) = \frac{1}{2}\ln\left(\frac{2(1+v)}{1+\sqrt{\xi}}\right)\ln\left(\frac{2+\sqrt{\xi}}{2}\right) + \frac{1}{4}\ln\left(\frac{2(1+\sqrt{\xi})}{1+v}\right)^2$$
$$- \ln^2 2 - \mathrm{Li}_2\left(\frac{2\sqrt{\xi}}{2+\sqrt{\xi}}\right) - \mathrm{Li}_2\left(\frac{1}{2}\right) - \mathrm{Li}_2\left(\frac{2+\sqrt{\xi}}{4}\right)$$
$$+ \mathrm{Li}_2\left(\frac{1-v+\sqrt{\xi}}{2+\sqrt{\xi}}\right) + \mathrm{Li}_2\left(\frac{\sqrt{\xi}}{1-v+\sqrt{\xi}}\right) + \mathrm{Li}_2\left(\frac{\sqrt{\xi}(2+\sqrt{\xi})}{2(1-v+\sqrt{\xi})}\right),$$

$$I_0^{L_0}(0) = \frac{1}{4}\ln\left(\frac{1+v}{1-v}\right)^2 + \mathrm{Li}_2\left(\frac{1-v}{2}\right) + \mathrm{Li}_2\left(\frac{1+v}{2}\right) - 2\mathrm{Li}_2\left(\frac{\sqrt{\xi}}{2}\right),$$

$$I_{t-}^{L_+}(0) = 2\mathrm{Li}_2\left(-\frac{1-v-\sqrt{\xi}}{1+v+\sqrt{\xi}}\right) - 2\mathrm{Li}_2\left(\frac{(2+\sqrt{\xi})(1-v-\sqrt{\xi})}{(1-v)(1-v+\sqrt{\xi})}\right)$$
$$- \mathrm{Li}_2\left(-\frac{1-v-\sqrt{\xi}}{1+v}\right) + \mathrm{Li}_2\left(\frac{1-v-\sqrt{\xi}}{1-v}\right) + \mathrm{Li}_2\left(\frac{2(1-v-\sqrt{\xi})}{(1-v)^2}\right),$$

$$I_{t+}^{L_+}(0) = \mathrm{Li}_2\left(\frac{-2v}{1-v}\right) - \mathrm{Li}_2\left(\frac{2v}{1+v}\right) - \mathrm{Li}_2\left(\frac{4v}{(1+v)^2}\right)$$
$$+ \mathrm{Li}_2\left(\frac{2(1+v-\sqrt{\xi})}{(1+v)^2}\right) - \mathrm{Li}_2\left(-\frac{1+v-\sqrt{\xi}}{1-v}\right) + \mathrm{Li}_2\left(\frac{1+v-\sqrt{\xi}}{1+v}\right)$$
$$- 2\mathrm{Li}_2\left(\frac{(2+\sqrt{\xi})(1+v-\sqrt{\xi})}{(1+v)(1+v+\sqrt{\xi})}\right) + 2\mathrm{Li}_2\left(\frac{2(2+\sqrt{\xi})v}{(1+v)(1+v+\sqrt{\xi})}\right)$$
$$+ 2\mathrm{Li}_2\left(-\frac{1+v-\sqrt{\xi}}{1-v+\sqrt{\xi}}\right) - 2\mathrm{Li}_2\left(\frac{-2v}{1-v+\sqrt{\xi}}\right),$$

$$I_{1-}^{L_+}(0) = -\mathrm{Li}_2\left(\frac{1-v-\sqrt{\xi}}{2-\sqrt{\xi}}\right) + \mathrm{Li}_2\left(-\frac{1-v-\sqrt{\xi}}{\sqrt{\xi}}\right) + \mathrm{Li}_2\left(-2\frac{1-v-\sqrt{\xi}}{\sqrt{\xi}(2-\sqrt{\xi})}\right)$$
$$- 2\mathrm{Li}_2\left(-\frac{(2+\sqrt{\xi})(1-v-\sqrt{\xi})}{2\sqrt{\xi}}\right) + 2\mathrm{Li}_2\left(\frac{1-v-\sqrt{\xi}}{2}\right),$$

$$I_{1+}^{L_+}(0) = \frac{1}{2}\ln\left(\frac{(2+\sqrt{\xi})^3}{8(1+\sqrt{\xi})^2}\right)\ln\left(\frac{2(1+v)}{1+\sqrt{\xi}}\right) - \mathrm{Li}_2\left(\frac{2\sqrt{\xi}}{2+\sqrt{\xi}}\right) - \mathrm{Li}_2\left(\frac{1}{2}\right)$$
$$- \mathrm{Li}_2\left(\frac{2+\sqrt{\xi}}{4}\right) + \mathrm{Li}_2\left(\frac{1-v+\sqrt{\xi}}{2+\sqrt{\xi}}\right) + \mathrm{Li}_2\left(\frac{\sqrt{\xi}}{1-v+\sqrt{\xi}}\right)$$
$$+ \mathrm{Li}_2\left(\frac{\sqrt{\xi}(2+\sqrt{\xi})}{2(1-v+\sqrt{\xi})}\right) + 2\mathrm{Li}_2\left(\frac{1+\sqrt{\xi}}{2+\sqrt{\xi}}\right) + 2\mathrm{Li}_2\left(\frac{\sqrt{\xi}}{1+\sqrt{\xi}}\right)$$
$$- 2\mathrm{Li}_2\left(\frac{2\sqrt{\xi}(1+\sqrt{\xi})}{(2+\sqrt{\xi})(1-v+\sqrt{\xi})}\right) - 2\mathrm{Li}_2\left(\frac{1-v+\sqrt{\xi}}{2(1+\sqrt{\xi})}\right),$$

$$I_0^{L_+}(0) = 4\mathrm{Li}_2\left(\frac{\sqrt{\xi}}{2+\sqrt{\xi}}\right) - 2\mathrm{Li}_2\left(\frac{1+v}{2+\sqrt{\xi}}\right) - 2\mathrm{Li}_2\left(\frac{1-v}{2+\sqrt{\xi}}\right)$$
$$+ \mathrm{Li}_2\left(\frac{1-v}{2}\right) + \mathrm{Li}_2\left(\frac{1+v}{2}\right) - 2\mathrm{Li}_2\left(\frac{\sqrt{\xi}}{2}\right). \tag{A6}$$

Still, not all of these integrals are independent of each other. Because

$$\frac{dy}{y} = \left(\frac{1}{t - t_-} + \frac{1}{t - t_+} - \frac{1}{t} \right) dt \tag{A7}$$

for the standard substitution $t = (1 - y - \sqrt{(1 - y)^2 - \xi})/\sqrt{\xi}$ used in this paper, and

$$L_0 = \int_{z_-}^{z_+} \frac{dz}{z}, \qquad L_\pm = -\int_{z_-}^{z_+} \frac{dz}{1 \pm \sqrt{\xi} - z}, \tag{A8}$$

using the symmetry of the phase space for $t\bar{t}$ pairs, one obtains

$$I_{t-}^{L_\pm}(0) + I_{t+}^{L_\pm}(0) - I_0^{L_\pm}(0) = \int_0^{1-\sqrt{\xi}} \int_{z_-(y)}^{z_+(y)} \frac{dz}{1 \pm \sqrt{\xi} - z} \frac{dy}{y}$$

$$= \int_0^{1-\sqrt{\xi}} \int_{z_-(y)}^{z_+(y)} \frac{dz}{z} \frac{dy}{1 \pm \sqrt{\xi} - y} = I_0^{L_0}(0) \mp 2I_{1\pm}^{L_0}(0), \tag{A9}$$

where for the last step we used

$$\frac{dy}{1 \pm \sqrt{\xi} - y} = \left(\frac{1}{t} \mp \frac{2}{1 \pm t} \right) dt. \tag{A10}$$

Using Eq. (A9) to eliminate $I_{1+}^{L_0}(0)$, we obtain the results presented in Appendix B. The relation also takes into account the integrals with $L_-(t)$ which are absent in our case. If such integrals appear in an intermediate step, they can be eliminated by using the relation

$$I_0^{L_+}(0) + 2I_{1-}^{L_+}(0) = -\int_0^{1-\sqrt{\xi}} \int_{z_-(y)}^{z_+(y)} \frac{dz}{1 + \sqrt{\xi} - z} \frac{dy}{1 - \sqrt{\xi} - y}$$

$$= -\int_0^{1-\sqrt{\xi}} \int_{z_-(y)}^{z_+(y)} \frac{dz}{1 - \sqrt{\xi} - z} \frac{dy}{1 + \sqrt{\xi} - y} = I_0^{L_-}(0) - 2I_{1+}^{L_-}(0). \tag{A11}$$

The nonappearance of $L_-(t)$ is related to the fact that there is no singularity at the upper boundary $y = 1 - \sqrt{\xi}$.

APPENDIX B: $O(\alpha_s)$ RESULTS

In this appendix we present our analytic results for the $O(\alpha_s)$ contributions to the correlation matrix in terms of the three unit vectors $\hat{t}$, $\hat{n}$ and $\hat{l}$ in the laboratory frame. The detailed results have to be combined with the electroweak form factors (cf. Ref. [12]) to obtain

$$\rho^{P_1 P_2} = \sum_{i,j=1}^4 g_{ij} \rho_{ij}^{P_1 P_2} \tag{B1}$$

$(P_1, P_2 \in \{t, n, l\})$. The general factor N is given in Eq. (54). Again, $\rho_{ij}^{P_1 P_2}$ is divided up into five different angular dependences,

$$\rho_{ij}^{P_1 P_2} = \frac{1}{4}(1 + \cos^2\theta)\rho_{ijU}^{P_1 P_2} + \frac{1}{2}\sin^2\theta \rho_{ijL}^{P_1 P_2} + \frac{1}{2}\cos\theta \rho_{ijF}^{P_1 P_2}$$

$$+ \frac{1}{2}\sin\theta \cos\theta \rho_{ijI}^{P_1 P_2} + \frac{1}{2}\sin\theta \rho_{ijA}^{P_1 P_2}, \tag{B2}$$

where the additional indices stand for unpolarized transverse (U), longitudinal (L), forward-/backward-asymmetric (F), longitudinal/transverse interference (I), and parity-asymmetric (A) components of the intermediate (γ or Z) boson. Our results read

$$\rho_{11U}^{tt} = N\Bigg[\frac{2v}{(1+\sqrt{\xi})\sqrt{\xi}}(4+8\sqrt{\xi}+13\xi+13\xi^{3/2})$$

$$+\frac{1}{(1+\sqrt{\xi})\sqrt{\xi}}(4+4\sqrt{\xi}-\xi-23\xi^{3/2}-12\xi^2-2\xi^{5/2})\ell_3$$

$$+\frac{\sqrt{\xi}}{4(1+\sqrt{\xi})^2}(176+369\sqrt{\xi}+320\xi+134\xi^{3/2}+24\xi^2+\xi^{5/2})I_0^{L_+}(0)$$

$$+\frac{8}{(1+\sqrt{\xi})v^2\xi}(1+3\sqrt{\xi}-\xi-\xi^{3/2})I_{1-}^{L_+}(0)+\frac{8}{\xi}(1+\sqrt{\xi})^4(1-2\sqrt{\xi})I_{1+}^{L_+}(0)$$

$$+\frac{(1+\sqrt{\xi})\sqrt{\xi}}{4(1-\sqrt{\xi})}(16-\sqrt{\xi}-12\xi+\xi^{3/2})(I_{t-}^{L_+}(0)+I_{t+}^{L_+}(0))$$

$$-\frac{(1-\sqrt{\xi})\sqrt{\xi}}{4(1+\sqrt{\xi})^2}(16+\sqrt{\xi}+\xi+7\xi^{3/2}-\xi^2)(I_0^{L_0}(0)+2I_{1-}^{L_0}(0))\Bigg],\tag{B3}$$

$$\rho_{11L}^{tt} = N\Bigg[-\frac{1}{2v\sqrt{\xi}}(20+20\sqrt{\xi}+65\xi+2\xi^{3/2}-105\xi^2-18\xi^{5/2})$$

$$-\frac{1}{4v^2\sqrt{\xi}}(20-101\xi-166\xi^{3/2}+143\xi^2+196\xi^{5/2}-2\xi^3-42\xi^{7/2})\ell_3$$

$$-\frac{\sqrt{\xi}}{16(1+\sqrt{\xi})^2}(896+2033\sqrt{\xi}+1932\xi+1006\xi^{3/2}+300\xi^2+41\xi^{5/2})I_0^{L_+}(0)$$

$$-\frac{2}{v^4\xi}(5+10\sqrt{\xi}-19\xi+12\xi^2)I_{1-}^{L_+}(0)-\frac{2}{\xi}(1+\sqrt{\xi})^4(5-10\sqrt{\xi}+\xi)I_{1+}^{L_+}(0)$$

$$-\frac{\xi}{16(1-\sqrt{\xi})^2}(47-72\sqrt{\xi}+122\xi-8\xi^{3/2}-57\xi^2)(I_{t-}^{L_+}(0)+I_{t+}^{L_+}(0))$$

$$-\frac{\xi}{16(1+\sqrt{\xi})^2}(271+196\sqrt{\xi}-78\xi-92\xi^{3/2}-41\xi^2)I_0^{L_0}(0)$$

$$-\frac{(1-\sqrt{\xi})\xi}{8(1+\sqrt{\xi})^2}(143+83\sqrt{\xi}-59\xi-23\xi^{3/2})I_{1-}^{L_0}(0)+4\xi((2-\xi)(\hat{I}_{t-}^{L_0}(0)+I_{t+}^{L_0}(0))-4v(\ell_0^-+\ell_0^+))\Bigg],\tag{B4}$$

$$\rho_{12U}^{tt} = N\Bigg[4v(6+3\sqrt{\xi}+4\xi)-2\sqrt{\xi}(2+4\sqrt{\xi}+\xi)\ell_3+\frac{2+\sqrt{\xi}}{1+\sqrt{\xi}}(8+12\sqrt{\xi}+18\xi+11\xi^{3/2}+3\xi^2)I_0^{L_+}(0)$$

$$+\frac{24}{v^2}I_{1-}^{L_+}(0)-8(1+\sqrt{\xi})^4I_{1+}^{L_+}(0)+\frac{(1+\sqrt{\xi})\xi}{1-\sqrt{\xi}}(4-\xi)(I_{t-}^{L_+}(0)+I_{t+}^{L_+}(0))$$

$$+\frac{\xi^{3/2}}{1+\sqrt{\xi}}(1-\sqrt{\xi})(2-\sqrt{\xi})(I_0^{L_0}(0)+2I_{1-}^{L_0}(0))\Bigg],\tag{B5}$$

$$\rho_{12U}^{tt} = N\Bigg[\frac{2\sqrt{\xi}}{v}(12+3\sqrt{\xi}-12\xi+\xi^{3/2})+\frac{1}{v^2}(20-4\sqrt{\xi}-46\xi+2\xi^{3/2}+11\xi^2+2\xi^{5/2}+3\xi^3)\ell_3$$

$$-\frac{1}{2(1+\sqrt{\xi})^2}(16+16\sqrt{\xi}-20\xi-59\xi^{3/2}-49\xi^2-15\xi^{5/2}-\xi^3)I_0^{L_+}(0)$$

$$-\frac{4}{v^4}(5-\xi)I_{1-}^{L_+}(0)-4(1+\sqrt{\xi})^4I_{1+}^{L_+}(0)-\frac{\xi}{2(1-\sqrt{\xi})^2}(16-13\sqrt{\xi}+\xi+3\xi^{3/2}-3\xi^2)(I_{t-}^{L_+}(0)+I_{t+}^{L_+}(0))$$

$$-\frac{1}{2(1+\sqrt{\xi})^2}(16+32\sqrt{\xi}+4\xi-9\xi^{3/2}-7\xi^2-5\xi^{5/2}+\xi^3)I_0^{L_0}(0)$$

$$+\frac{(1-\sqrt{\xi})\xi}{(1+\sqrt{\xi})^2}(4-3\sqrt{\xi}-4\xi+\xi^{3/2})I_{1-}^{L_0}(0)+4((2-\xi)(\hat{I}_{t-}^{L_0}(0)+I_{t+}^{L_0}(0))-4v(\ell_0^-+\ell_0^+))\Bigg],\tag{B6}$$

$$\rho_{44F}^{tt} = N\left[-\frac{4\sqrt{\xi}}{1+\sqrt{\xi}}(6-8\sqrt{\xi}-5\xi+3\xi^{3/2}) - \frac{4}{v^2}(4-4\sqrt{\xi}+3\xi^{3/2}+\xi^2)\ell_1\right.$$

$$-\frac{2(1+\sqrt{\xi})}{1-\sqrt{\xi}}(4-\xi)(2-\sqrt{\xi})\ell_2 + \frac{2v\sqrt{\xi}}{(1+\sqrt{\xi})^2}(20+30\sqrt{\xi}+19\xi+9\xi^{3/2}+3\xi^2)\ell_3$$

$$+\frac{(2+\sqrt{\xi})^2\sqrt{\xi}}{(1+\sqrt{\xi})^2}(4+3\sqrt{\xi}+2\xi)I_0^{L_+}(0) - \frac{v\xi^2}{(1-\sqrt{\xi})^2}(I_{t-}^{L_+}(0)+I_{t+}^{L_+}(0))$$

$$\left.-\frac{\sqrt{\xi}}{(1+\sqrt{\xi})^2}(8+12\sqrt{\xi}+24\xi+27\xi^{3/2}+10\xi^2)I_0^{L_0}(0)\right], \tag{B7}$$

$$\rho_{13U}^{tn} = N\left[-\frac{4}{1+\sqrt{\xi}}(6-3\sqrt{\xi}-5\xi+4\xi^{3/2}-6\xi^2) - \frac{4}{v^2}(12+8\sqrt{\xi}-4\xi-9\xi^{3/2}-3\xi^2)\ell_1\right.$$

$$-\frac{2}{1-\sqrt{\xi}}(24-16\sqrt{\xi}+6\xi-10\xi^{3/2}-\xi^2+3\xi^{5/2})\ell_2 - \frac{2v\xi}{(1+\sqrt{\xi})^2}(6-\sqrt{\xi}-\xi+3\xi^{3/2})\ell_3$$

$$-\frac{2+\sqrt{\xi}}{(1+\sqrt{\xi})^2}(8+20\sqrt{\xi}+30\xi+21\xi^{3/2}+6\xi^2)I_0^{L_+}(0)$$

$$\left.-\frac{v\xi}{(1-\sqrt{\xi})^2}(4-3\xi)(I_{t-}^{L_+}(0)-I_{t+}^{L_+}(0)) - \frac{\xi^{3/2}}{(1+\sqrt{\xi})^2}(6-5\sqrt{\xi}-8\xi)I_0^{L_0}(0)\right], \tag{B8}$$

$$\rho_{13L}^{tn} = N\left[-\frac{2\sqrt{\xi}}{1+\sqrt{\xi}}(16-2\sqrt{\xi}-21\xi+3\xi^{3/2}) - \frac{2}{v^2}(4+12\sqrt{\xi}-4\xi-7\xi^{3/2}-\xi^2)\ell_1\right.$$

$$+\frac{1}{1-\sqrt{\xi}}(8-28\sqrt{\xi}+10\xi+5\xi^{3/2}-\xi^2)\ell_2 + \frac{v}{(1+\sqrt{\xi})^2}(4+8\sqrt{\xi}-2\xi-23\xi^{3/2}-11\xi^2+3\xi^{5/2})\ell_3$$

$$-\frac{(2+\sqrt{\xi})^2}{2(1+\sqrt{\xi})^2}(4+16\sqrt{\xi}+17\xi+8\xi^{3/2})I_0^{L_+}(0) - \frac{v\xi}{2(1-\sqrt{\xi})^2}(12-4\sqrt{\xi}-7\xi)(I_{t-}^{L_+}(0)-I_{t+}^{L_+}(0))$$

$$\left.-\frac{1}{2(1+\sqrt{\xi})^2}(16+32\sqrt{\xi}-8\xi-52\xi^{3/2}-17\xi^2+8\xi^{5/2})I_0^{L_0}(0) + 4v((2-\xi)(\hat{I}_{t-}^{L_0}(0)-I_{t+}^{L_0}(0))-4v\ell_0^-)\right], \tag{B9}$$

$$\rho_{14L}^{tn} = 4N\pi v\xi, \tag{B10}$$

$$\rho_{11I}^{tl} = N\left[-\frac{1}{v\sqrt{\xi}}(16+16\sqrt{\xi}+20\xi-12\xi^{3/2}-55\xi^2-4\xi^{5/2}+3\xi^3)\right.$$

$$-\frac{1}{2v^2\sqrt{\xi}}(16-4\xi-24\xi^{3/2}+26\xi^2+28\xi^{5/2}+7\xi^3-4\xi^{7/2}+3\xi^4)\ell_3$$

$$-\frac{\sqrt{\xi}}{2(1+\sqrt{\xi})^2}(152+303\sqrt{\xi}+211\xi+51\xi^{3/2}-3\xi^2-2\xi^{5/2})I_0^{L_+}(0)$$

$$-\frac{8}{v^4\xi}(2+4\sqrt{\xi}-7\xi+5\xi^2)I_{1-}^{L_+}(0) - \frac{8}{\xi}(1+\sqrt{\xi})^4(2-4\sqrt{\xi}+\xi)I_{1+}^{L_+}(0)$$

$$-\frac{\sqrt{\xi}}{2(1-\sqrt{\xi})^2}(8+25\sqrt{\xi}-39\xi+9\xi^{3/2}+11\xi^2-6\xi^{5/2})(I_{t-}^{L_+}(0)+I_{t+}^{L_+}(0))$$

$$+\frac{\sqrt{\xi}}{2(1+\sqrt{\xi})^2}(24+15\sqrt{\xi}+9\xi-\xi^{3/2}-13\xi^2-2\xi^{5/2})I_0^{L_0}(0)$$

$$+\frac{(1-\sqrt{\xi})^2\sqrt{\xi}}{(1+\sqrt{\xi})^2}(8-\sqrt{\xi}-9\xi-2\xi^{3/2})I_{1-}^{L_0}(0)$$

$$\left.-4\sqrt{\xi}((2-\xi)(\hat{I}_{t-}^{L_0}(0)+I_{t+}^{L_0}(0))-4v(\ell_0^-+\ell_0^+))\right], \tag{B11}$$

$$\rho_{12I}^{tl} = N\left[-\frac{1}{v}(64 - 4\sqrt{\xi} - 84\xi + 7\xi^{3/2} + 4\xi^2 - 3\xi^{5/2})\right.$$

$$-\frac{\sqrt{\xi}}{2v^2}(40 + 64\sqrt{\xi} - 74\xi - 20\xi^{3/2} + 37\xi^2 + 4\xi^{5/2} - 3\xi^3)\ell_3$$

$$-\frac{1}{2(1+\sqrt{\xi})^2}(64 + 160\sqrt{\xi} + 212\xi + 159\xi^{3/2} + 65\xi^2 + 17\xi^{5/2} + 3\xi^3)I_0^{L_+}(0)$$

$$-\frac{8}{v^4}(7 - 3\xi)I_{1-}^{L_+}(0) + 8(1+\sqrt{\xi})^4 I_{1+}^{L_+}(0)$$

$$-\frac{\xi}{2(1-\sqrt{\xi})^2}(52 - 31\sqrt{\xi} - 29\xi + 11\xi^{3/2} + 5\xi^2)(I_{t-}^{L_+}(0) + I_{t+}^{L_+}(0))$$

$$+\frac{\sqrt{\xi}}{2(1+\sqrt{\xi})^2}(16 + 52\sqrt{\xi} - 3\xi - 35\xi^{3/2} - \xi^2 + 3\xi^{5/2})I_0^{L_0}(0)$$

$$+\frac{(1-\sqrt{\xi})\xi}{(1+\sqrt{\xi})^2}(20 + 9\sqrt{\xi} - 10\xi - 3\xi^{3/2})I_{1-}^{L_0}(0)$$

$$\left. -4\sqrt{\xi}((2-\xi)(\hat{I}_{t-}^{L_0}(0) + I_{t+}^{L_0}(0)) - 4v(\ell_0^- + \ell_0^+))\right], \tag{B12}$$

$$\rho_{43A}^{tl} = 2N\pi v\sqrt{\xi}(1+\xi), \tag{B13}$$

$$\rho_{44A}^{tl} = N\left[\frac{\sqrt{\xi}}{1+\sqrt{\xi}}(24 - 10\sqrt{\xi} - 7\xi + 6\xi^{3/2} + 3\xi^2) + \frac{4}{v^2}(4 - 5\xi^{3/2} - 3\xi^2)\ell_1\right.$$

$$+\frac{1}{2(1-\sqrt{\xi})}(32 + 8\sqrt{\xi} - 80\xi - 6\xi^{3/2} + 22\xi^2 + 3\xi^{5/2} - 3\xi^3)\ell_2$$

$$-\frac{2v\sqrt{\xi}}{(1+\sqrt{\xi})^2}(21 + 32\sqrt{\xi} + 12\xi - 5\xi^{3/2} - 3\xi^2)\ell_3$$

$$-\frac{(2+\sqrt{\xi})\sqrt{\xi}}{(1+\sqrt{\xi})^2}(8 + 10\sqrt{\xi} + 5\xi)I_0^{L_+}(0)$$

$$-\frac{v\xi}{(1-\sqrt{\xi})^2}(8 - 4\sqrt{\xi} - 3\xi)(I_{t-}^{L_+}(0) - I_{t+}^{L_+}(0))$$

$$+\frac{\sqrt{\xi}}{(1+\sqrt{\xi})^2}(16 + 28\sqrt{\xi} + 17\xi - \xi^{3/2} - 3\xi^2)I_0^{L_0}(0)$$

$$\left. -4v\sqrt{\xi}((2-\xi)(\hat{I}_{t-}^{L_0}(0) - I_{t+}^{L_0}(0)) - 4v\ell_0^-)\right], \tag{B14}$$

$$\rho_{13U}^{nt} = N\left[\frac{4}{1+\sqrt{\xi}}(6 - 3\sqrt{\xi} - 5\xi + 4\xi^{3/2} - 6\xi^2) + \frac{4}{v^2}(12 + 8\sqrt{\xi} - 4\xi - 9\xi^{3/2} - 3\xi^2)\ell_1\right.$$

$$+\frac{2}{1-\sqrt{\xi}}(24 - 16\sqrt{\xi} + 6\xi - 10\xi^{3/2} - \xi^2 + 3\xi^{5/2})\ell_2$$

$$+\frac{2v\xi}{(1+\sqrt{\xi})^2}(6 - \sqrt{\xi} - \xi + 3\xi^{3/2})\ell_3$$

$$+\frac{2+\sqrt{\xi}}{(1+\sqrt{\xi})^2}(8 + 20\sqrt{\xi} + 30\xi + 21\xi^{3/2} + 6\xi^2)I_0^{L_+}(0)$$

$$\left. +\frac{v\xi}{(1-\sqrt{\xi})^2}(4 - 3\xi)(I_{t-}^{L_+}(0) - I_{t+}^{L_+}(0)) + \frac{\xi^{3/2}}{(1+\sqrt{\xi})^2}(6 - 5\sqrt{\xi} - 8\xi)I_0^{L_0}(0)\right], \tag{B15}$$

$$\rho^{nt}_{13L} = N\Bigg[\frac{2\sqrt{\xi}}{1+\sqrt{\xi}}(20+10\sqrt{\xi}-19\xi+9\xi^{3/2})-\frac{2}{v^2}(20-4\sqrt{\xi}-4\xi+5\xi^{3/2}+3\xi^2)\ell_1$$

$$-\frac{1}{(1-\sqrt{\xi})}(24-36\sqrt{\xi}+46\xi+3\xi^{3/2}-7\xi^2)\ell_2$$

$$+\frac{v}{(1+\sqrt{\xi})^2}(4+8\sqrt{\xi}-42\xi-51\xi^{3/2}-23\xi^2-9\xi^{5/2})\ell_3$$

$$-\frac{(2+\sqrt{\xi})^2}{2(1+\sqrt{\xi})^2}(4+5\xi)I_0^{L_+}(0)-\frac{v\xi}{2(1-\sqrt{\xi})^2}(12-4\sqrt{\xi}-3\xi)(I_{t-}^{L_+}(0)-I_{t+}^{L_+}(0))$$

$$-\frac{1}{2(1+\sqrt{\xi})^2}(16+32\sqrt{\xi}-24\xi-60\xi^{3/2}-53\xi^2-24\xi^{5/2})I_0^{L_0}(0)$$

$$+4v((2-\xi)(\hat{I}_{t-}^{L_0}(0)-I_{t+}^{L_0}(0))-4v\ell_0^-)\Bigg], \tag{B16}$$

$$\rho^{nt}_{14L}=4N\pi v\xi, \tag{B17}$$

$$\rho^{nn}_{11U}=N\Bigg[\frac{2v}{(1+\sqrt{\xi})\sqrt{\xi}}(4+8\sqrt{\xi}+13\xi+13\xi^{3/2})$$

$$+\frac{1}{(1+\sqrt{\xi})\sqrt{\xi}}(4+4\sqrt{\xi}-\xi-23\xi^{3/2}-12\xi^2-2\xi^{5/2})\ell_3$$

$$+\frac{\sqrt{\xi}}{4(1+\sqrt{\xi})^2}(176+369\sqrt{\xi}+320\xi+134\xi^{3/2}+24\xi^2+\xi^{5/2})I_0^{L_+}(0)$$

$$+\frac{8}{(1+\sqrt{\xi})v^2\xi}(1+3\sqrt{\xi}-\xi-\xi^{3/2})I_{1-}^{L_+}(0)$$

$$+\frac{8}{\xi}(1+\sqrt{\xi})^4(1-2\sqrt{\xi})I_{1+}^{L_+}(0)$$

$$+\frac{(1+\sqrt{\xi})\sqrt{\xi}}{4(1-\sqrt{\xi})}(16-\sqrt{\xi}-12\xi+\xi^{3/2})(I_{t-}^{L_+}(0)+I_{t+}^{L_+}(0))$$

$$-\frac{(1-\sqrt{\xi})\sqrt{\xi}}{4(1+\sqrt{\xi})^2}(16+\sqrt{\xi}+\xi+7\xi^{3/2}-\xi^2)(I_0^{L_0}(0)+2I_{1-}^{L_0}(0))\Bigg], \tag{B18}$$

$$\rho^{nn}_{11L}=N\Bigg[-\frac{v}{2(1+\sqrt{\xi})\sqrt{\xi}}(12+24\sqrt{\xi}+79\xi+77\xi^{3/2}-2\xi^2)$$

$$-\frac{1}{4(1+\sqrt{\xi})\sqrt{\xi}}(12+12\sqrt{\xi}-55\xi-129\xi^{3/2}-32\xi^2+12\xi^{5/2}+6\xi^3)\ell_3$$

$$-\frac{\sqrt{\xi}}{16(1+\sqrt{\xi})^2}(640+1463\sqrt{\xi}+1396\xi+650\xi^{3/2}+132\xi^2+7\xi^{5/2})I_0^{L_+}(0)$$

$$-\frac{2}{(1+\sqrt{\xi})v^2\xi}(3+9\sqrt{\xi}-4\xi-4\xi^{3/2})I_{1-}^{L_+}(0)-\frac{2}{\xi}(1+\sqrt{\xi})^4(3-6\sqrt{\xi}-\xi)I_{1+}^{L_+}(0)$$

$$-\frac{(1+\sqrt{\xi})\xi}{16(1-\sqrt{\xi})}(41-24\sqrt{\xi}-9\xi)(I_{t-}^{L_+}(0)+I_{t+}^{L_+}(0))$$

$$-\frac{(1-\sqrt{\xi})\xi}{16(1+\sqrt{\xi})^2}(73+5\sqrt{\xi}-37\xi+7\xi^{3/2})(I_0^{L_0}(0)+2I_{1-}^{L_0}(0))\Bigg], \tag{B19}$$

$$\rho_{12U}^{nn} = N\left[4v(6 + 3\sqrt{\xi} + 4\xi) - \sqrt{\xi}(2 + 4\sqrt{\xi} + \xi)\ell_3\right.$$

$$+ \frac{2 + \sqrt{\xi}}{1 + \sqrt{\xi}}(8 + 12\sqrt{\xi} + 18\xi + 11\xi^{3/2} + 3\xi^2)I_0^{L_+}(0)$$

$$+ \frac{24}{v^2}I_{1-}^{L_+}(0) - 8(1 + \sqrt{\xi})^4 I_{1+}^{L_+}(0) - \frac{(1 + \sqrt{\xi})\xi}{1 - \sqrt{\xi}}(4 - \xi)(I_{t-}^{L_+}(0) + I_{t+}^{L_+}(0))$$

$$+ \left. \frac{\xi^{3/2}}{1 + \sqrt{\xi}}(1 - \sqrt{\xi})(2 - \sqrt{\xi})(I_0^{L_0}(0) + 2I_{1-}^{L_0}(0))\right], \tag{B20}$$

$$\rho_{12L}^{nn} = N\left[2v\sqrt{\xi}(8 - 7\sqrt{\xi}) - (20 + 4\sqrt{\xi} - 42\xi + 4\xi^{3/2} + 13\xi^2)\ell_3\right.$$

$$+ \frac{1}{2(1 + \sqrt{\xi})}(16 + 64\sqrt{\xi} + 100\xi + 61\xi^{3/2} + 9\xi^2 - 2\xi^{5/2})I_0^{L_+}(0)$$

$$+ \frac{4}{v^2}I_{1-}^{L_+}(0) - 12(1 + \sqrt{\xi})^4 I_{1+}^{L_+}(0) + \frac{(1 + \sqrt{\xi})\xi}{2(1 - \sqrt{\xi})}(24 - 9\sqrt{\xi} - 14\xi)(I_{t-}^{L_+}(0) + I_{t+}^{L_+}(0))$$

$$+ \frac{1 - \sqrt{\xi}}{2(1 + \sqrt{\xi})}(16 + 32\sqrt{\xi} - 4\xi - 21\xi^{3/2} - 2\xi^2)I_0^{L_0}(0)$$

$$- \left. \frac{(1 - \sqrt{\xi})\xi}{1 + \sqrt{\xi}}(12 + 5\sqrt{\xi} - 6\xi)I_{1-}^{L_0}(0) - 4v^2((2 - \xi)(\hat{I}_{t-}^{L_0}(0) + I_{t+}^{L_0}(0)) - 4v(\ell_0^- + \ell_0^+))\right], \tag{B21}$$

$$\rho_{44F}^{nn} = N\left[-\frac{4\sqrt{\xi}}{1 + \sqrt{\xi}}(6 - 8\sqrt{\xi} - 5\xi + 3\xi^{3/2}) - \frac{4}{v^2}(4 - 4\sqrt{\xi} + 3\xi^{3/2} + \xi^2)\ell_1\right.$$

$$- \frac{2(1 + \sqrt{\xi})}{1 - \sqrt{\xi}}(8 - 4\sqrt{\xi} - 2\xi + \xi^{3/2})\ell_2 + \frac{2v\sqrt{\xi}}{(1 + \sqrt{\xi})^2}(20 + 30\sqrt{\xi} + 19\xi + 9\xi^{3/2} + 3\xi^2)\ell_3$$

$$+ \frac{\sqrt{\xi}}{(1 + \sqrt{\xi})^2}(16 + 28\sqrt{\xi} + 24\xi + 11\xi^{3/2} + 2\xi^2)I_0^{L_+}(0)$$

$$- \left. \frac{\sqrt{\xi}}{(1 + \sqrt{\xi})^2}(8 + 12\sqrt{\xi} + 24\xi + 27\xi^{3/2} + 10\xi^2)I_0^{L_0}(0) - \frac{v\xi^2}{(1 - \sqrt{\xi})^2}(I_{t-}^{L_+}(0) - I_{t+}^{L_+}(0))\right], \tag{B22}$$

$$\rho_{13I}^{nl} = N\left[-\frac{1}{1 + \sqrt{\xi}}(64 - 52\sqrt{\xi} - 114\xi + 45\xi^{3/2} - 26\xi^2 + 3\xi^{5/2})\right.$$

$$- \frac{4}{v^2}(28 + 8\sqrt{\xi} - 8\xi - 7\xi^{3/2} - \xi^2)\ell_1$$

$$- \frac{1}{2(1 - \sqrt{\xi})}(224 - 168\sqrt{\xi} + 48\xi + 14\xi^{3/2} + 2\xi^2 + 3\xi^{5/2} - 3\xi^3)\ell_2$$

$$- \frac{2v\sqrt{\xi}}{(1 + \sqrt{\xi})^2}(1 + 40\sqrt{\xi} + 32\xi + 7\xi^{3/2} + 5\xi^2)\ell_3$$

$$- \frac{2 + \sqrt{\xi}}{(1 + \sqrt{\xi})^2}(16 + 32\sqrt{\xi} + 50\xi + 33\xi^{3/2} + 8\xi^2)I_0^{L_+}(0)$$

$$+ \frac{\sqrt{\xi}}{(1 + \sqrt{\xi})^2}(8 + 36\sqrt{\xi} + 17\xi + 11\xi^{3/2} + 13\xi^2)I_0^{L_0}(0)$$

$$- \frac{v\xi}{(1 - \sqrt{\xi})^2}(16 - 4\sqrt{\xi} - 7\xi)(I_{t-}^{L_+}(0) - I_{t+}^{L_+}(0))$$

$$- \left. 4v\sqrt{\xi}((2 - \xi)(\hat{I}_{t-}^{L_0}(0) - I_{t+}^{L_0}(0)) - 4v\ell_0^-)\right], \tag{B23}$$

$$\rho_{14I}^{nl} = -2N\pi v\sqrt{\xi}(1+\xi), \tag{B24}$$

$$\rho_{41A}^{nl} = -2N\pi v^2\sqrt{\xi}, \tag{B25}$$

$$\rho_{42A}^{nl} = -2N\pi v^2\sqrt{\xi}, \tag{B26}$$

$$
\begin{aligned}
\rho_{11I}^{lt} = N\Bigg[&\frac{1}{v}(48 + 16\sqrt{\xi} - 40\xi + 3\xi^{3/2} - 32\xi^2 - 3\xi^{5/2}) - \frac{\sqrt{\xi}}{2v^2}(56 - 8\sqrt{\xi} + 2\xi - 72\xi^{3/2} - 13\xi^2 + 8\xi^{5/2} + 3\xi^3)\ell_3 \\
&+ \frac{2+\sqrt{\xi}}{2(1+\sqrt{\xi})^2}(32 + 62\sqrt{\xi} + 121\xi + 122\xi^{3/2} + 61\xi^2 + 10\xi^{5/2})I_0^{L_+}(0) \\
&+ \frac{16}{v^4}(3 - 2\sqrt{\xi})I_{1-}^{L_+}(0) - 16(1+\sqrt{\xi})^4 I_{1+}^{L_+}(0) + \frac{(2-\sqrt{\xi})\sqrt{\xi}}{2(1-\sqrt{\xi})^2}(2 + \sqrt{\xi} + 10\xi - 3\xi^{3/2} - 6\xi^2)(I_{t-}^{L_+}(0) + I_{t+}^{L_+}(0)) \\
&+ \frac{\sqrt{\xi}}{2(1+\sqrt{\xi})^2}(20 + 8\sqrt{\xi} + 25\xi - 4\xi^{3/2} - 19\xi^2 + 2\xi^{5/2})I_0^{L_0}(0) \\
&+ \frac{(1-\sqrt{\xi})\sqrt{\xi}}{(1+\sqrt{\xi})^2}(4 - 20\sqrt{\xi} - 3\xi + 9\xi^{3/2} - 2\xi^2)I_{1-}^{L_0}(0) - 4\sqrt{\xi}((2-\xi)(\hat{I}_{t-}^{L_0}(0) + \hat{I}_{t+}^{L_0}(0)) - 4v(\ell_0^- + \ell_0^+))\Bigg], \tag{B27}
\end{aligned}
$$

$$
\begin{aligned}
\rho_{12I}^{lt} = N\sqrt{\xi}\Bigg[&-\frac{\sqrt{\xi}}{v}(20 + 19\sqrt{\xi} - 28\xi - 3\xi^{3/2}) - \frac{1}{2v^2}(32 - 122\xi + 28\xi^{3/2} + 45\xi^2 - 4\xi^{5/2} - 3\xi^3)\ell_3 \\
&+ \frac{1}{2(1+\sqrt{\xi})^2}(32 + 40\sqrt{\xi} + 15\xi - 26\xi^{3/2} - 29\xi^2 - 8\xi^{5/2})I_0^{L_+}(0) + \frac{16}{v^4}(2 - \sqrt{\xi})I_{1-}^{L_+}(0) \\
&+ \frac{\sqrt{\xi}}{2(1-\sqrt{\xi})^2}(8 + 17\sqrt{\xi} - 26\xi - 3\xi^{3/2} + 8\xi^2)(I_{t-}^{L_+}(0) + I_{t+}^{L_+}(0)) \\
&+ \frac{1}{2(1+\sqrt{\xi})^2}(16 + 40\sqrt{\xi} - 5\xi - 14\xi^{3/2} - \xi^2 - 4\xi^{5/2})I_0^{L_0}(0) \\
&+ \frac{(1-\sqrt{\xi})\sqrt{\xi}}{(1+\sqrt{\xi})^2}(8 - 5\sqrt{\xi} - 3\xi + 4\xi^{3/2})I_{1-}^{L_0}(0) - 4((2-\xi)(\hat{I}_{t-}^{L_0}(0) + I_{t+}^{L_0}(0)) - 4v(\ell_0^- + \ell_0^+))\Bigg], \tag{B28}
\end{aligned}
$$

$$\rho_{43A}^{lt} = 2N\pi v\sqrt{\xi}(1+\xi), \tag{B29}$$

$$
\begin{aligned}
\rho_{44A}^{lt} = N\Bigg[&-\frac{1}{1+\sqrt{\xi}}(8 + 32\xi - 5\xi^{3/2} - 6\xi^2 + 3\xi^{5/2}) \\
&+ \frac{2}{v^2}(8 - 2\sqrt{\xi} + 10\xi + \xi^{3/2} - \xi^2)\ell_1 + \frac{4-\xi}{2(1-\sqrt{\xi})}(8 - 16\sqrt{\xi} + 8\xi + 19\xi^{3/2} - 3\xi^2)\ell_2 \\
&- \frac{v\sqrt{\xi}}{(1+\sqrt{\xi})^2}(6 - 44\sqrt{\xi} - 75\xi - 42\xi^{3/2} - 8\xi^2)\ell_3 \\
&- \frac{\sqrt{\xi}}{2(1+\sqrt{\xi})^2}(16 - 16\sqrt{\xi} - 70\xi - 76\xi^{3/2} - 35\xi^2 - 6\xi^{5/2})I_0^{L_+}(0) \\
&+ \frac{v\xi^{3/2}}{(1-\sqrt{\xi})^2}(7 - 2\sqrt{\xi} - 3\xi)(I_{t-}^{L_+}(0) - I_{t+}^{L_+}(0)) \\
&+ \frac{\sqrt{\xi}}{2(1+\sqrt{\xi})^2}(16 - 8\sqrt{\xi} - 56\xi - 72\xi^{3/2} - 37\xi^2 - 6\xi^{5/2})I_0^{L_0}(0) \\
&- 4v\sqrt{\xi}((2-\xi)(\hat{I}_{t-}^{L_0}(0) - I_{t+}^{L_0}(0)) - 4v\ell_0^-)\Bigg], \tag{B30}
\end{aligned}
$$

$$\rho_{13I}^{ln} = N\left[\frac{(1-\sqrt{\xi})\sqrt{\xi}}{1+\sqrt{\xi}}(24 + 40\sqrt{\xi} - 5\xi - 3\xi^{3/2}) - \frac{2}{1+\sqrt{\xi}}(8 - 10\sqrt{\xi} - 16\xi - 7\xi^{3/2})\ell_1\right.$$

$$-\frac{1}{2}(32 - 32\sqrt{\xi} + 40\xi + 20\xi^{3/2} - 16\xi^2 - 3\xi^{5/2})\ell_2 + \frac{v\sqrt{\xi}}{(1+\sqrt{\xi})^2}(2 + 53\xi + 62\xi^{3/2} + 16\xi^2)\ell_3$$

$$+\frac{\sqrt{\xi}}{2(1+\sqrt{\xi})^2}(48 + 112\sqrt{\xi} + 146\xi + 108\xi^{3/2} + 41\xi^2 + 6\xi^{5/2})I_0^{L_+}(0)$$

$$+\frac{\sqrt{\xi}}{2(1+\sqrt{\xi})^2}(16 + 32\sqrt{\xi} - 48\xi - 88\xi^{3/2} - 39\xi^2 - 6\xi^{5/2})I_0^{L_0}(0)$$

$$\left.+\frac{(1+\sqrt{\xi})\xi^{3/2}}{v}(5 + 3\sqrt{\xi})(I_{t-}^{L_+}(0) - I_{t+}^{L_+}(0)) - 4v\sqrt{\xi}((2-\xi)(\hat{I}_{t-}^{L_0}(0) - I_{t+}^{L_0}(0)) - 4v\ell_0^-)\right], \tag{B31}$$

$$\rho_{14I}^{ln} = -2N\pi v\sqrt{\xi}(1+\xi), \tag{B32}$$

$$\rho_{41A}^{ln} = -2N\pi v^2\sqrt{\xi}, \tag{B33}$$

$$\rho_{42A}^{ln} = -2N\pi v^2\sqrt{\xi}, \tag{B34}$$

$$\rho_{11U}^{ll} = N\left[\frac{2}{v}(10 - 12\sqrt{\xi} - 15\xi + 20\xi^{3/2} - 11\xi^2) + \frac{1}{v^2}(48 + 24\sqrt{\xi} - 52\xi - 60\xi^{3/2} + 55\xi^2 + 12\xi^{5/2} - 3\xi^3)\ell_3\right.$$

$$+\frac{1}{(1+\sqrt{\xi})^2}(32 + 54\sqrt{\xi} + 78\xi + 90\xi^{3/2} + 71\xi^2 + 30\xi^{5/2} + 5\xi^3)I_0^{L_+}(0)$$

$$+\frac{16}{v^4}(3 - 2\sqrt{\xi} + \xi)I_{1-}^{L_+}(0) - 16(1 + \sqrt{\xi})^4 I_{1+}^{L_+}(0)$$

$$+\frac{\sqrt{\xi}}{(1-\sqrt{\xi})^2}(26 - 14\sqrt{\xi} - 18\xi + \xi^{3/2} + 6\xi^2 + 3\xi^{5/2})(I_{t-}^{L_+}(0) + I_{t+}^{L_+}(0))$$

$$-\frac{1}{(1+\sqrt{\xi})^2}(16 + 22\sqrt{\xi} + 2\xi - 34\xi^{3/2} - 3\xi^2 + 14\xi^{5/2} - \xi^3)I_0^{L_0}(0)$$

$$+\frac{2(1-\sqrt{\xi})\sqrt{\xi}}{(1+\sqrt{\xi})^2}(10 + 8\sqrt{\xi} + 10\xi + \xi^{3/2} - 5\xi^2)I_{1-}^{L_0}(0)$$

$$\left.+4(2-\xi)((2-\xi)(\hat{I}_{t-}^{L_0}(0) + I_{t+}^{L_0}(0)) - 4v(\ell_0^- + \ell_0^+))\right], \tag{B35}$$

$$\rho_{11L}^{ll} = N\left[-\frac{1}{2v}(96 + 32\sqrt{\xi} - 50\xi - 97\xi^2 + 3\xi^3) + \frac{\sqrt{\xi}}{4v^2}(32 - 40\sqrt{\xi} + 88\xi - 104\xi^{3/2} - 24\xi^2 + 3\xi^{5/2} - 3\xi^{7/2})\ell_3\right.$$

$$-\frac{1}{2(1+\sqrt{\xi})^2}(64 + 156\sqrt{\xi} + 296\xi + 340\xi^{3/2} + 217\xi^2 + 70\xi^{5/2} + 9\xi^3)I_0^{L_+}(0)$$

$$-\frac{16}{v^4}(3 - 2\sqrt{\xi})I_{1-}^{L_+}(0) + 16(1 + \sqrt{\xi})^4 I_{1+}^{L_+}(0)$$

$$-\frac{\sqrt{\xi}}{2(1-\sqrt{\xi})^2}(4 + 8\sqrt{\xi} + 12\xi - 25\xi^{3/2} - 2\xi^2 + 7\xi^{5/2})(I_{t-}^{L_+}(0) + I_{t+}^{L_+}(0))$$

$$-\frac{\sqrt{\xi}}{2(1+\sqrt{\xi})^2}(4 - 24\sqrt{\xi} + 4\xi - 5\xi^{3/2} - 6\xi^2 + 11\xi^{5/2})I_0^{L_0}(0)$$

$$\left.-\frac{(1-\sqrt{\xi})^2\sqrt{\xi}}{(1+\sqrt{\xi})^2}(4 - 8\sqrt{\xi} + 7\xi^{3/2})I_{1-}^{L_0}(0) - \xi((2-\xi)(\hat{I}_{t-}^{L_0}(0) + I_{t+}^{L_0}(0)) - 4v(\ell_0^- + \ell_0^+))\right], \tag{B36}$$

$$\rho_{12U}^{ll} = N \left[\frac{4\sqrt{\xi}}{v} (16 + \sqrt{\xi} - 20\xi - \xi^{3/2}) - \frac{2\sqrt{\xi}}{v^2} (4 - 16\xi + 3\xi^{3/2} - 3\xi^{5/2})\ell_3 \right.$$

$$+ \frac{\sqrt{\xi}}{(1+\sqrt{\xi})^2} (48 + 134\sqrt{\xi} + 166\xi + 99\xi^{3/2} + 24\xi^2 + \xi^{5/2})I_0^{L_+}(0)$$

$$- \frac{16}{v^4} (1 - 2\sqrt{\xi} - \xi)I_{1-}^{L_+}(0) - 16(1 + \sqrt{\xi})^4 I_{1+}^{L_+}(0)$$

$$+ \frac{\xi}{(1-\sqrt{\xi})^2} (2 + 18\sqrt{\xi} - 19\xi - 4\xi^{3/2} + 7\xi^2)(I_{t-}^{L_+}(0) + I_{t+}^{L_+}(0))$$

$$- \frac{\xi}{(1+\sqrt{\xi})^2} (6 + 22\sqrt{\xi} + \xi - 12\xi^{3/2} - \xi^2)I_0^{L_0}(0)$$

$$\left. + \frac{2(1-\sqrt{\xi})^2\xi}{(1+\sqrt{\xi})^2} (2 - 2\sqrt{\xi} - 3\xi)I_{1-}^{L_0}(0) + 4\xi((2-\xi)(\hat{I}_{t-}^{L_0}(0) + I_{t+}^{L_0}(0)) - 4v(\ell_0^- + \ell_0^+)) \right], \tag{B37}$$

$$\rho_{12L}^{ll} = N \left[\frac{\xi}{2v} (70 + 32\sqrt{\xi} - 89\xi + 3\xi^2) - \frac{\sqrt{\xi}}{4v^2} (32 + 104\sqrt{\xi} + 104\xi - 176\xi^{3/2} - 40\xi^2 + 27\xi^{5/2} - 3\xi^{7/2})\ell_3 \right.$$

$$+ \frac{\sqrt{\xi}}{2(1+\sqrt{\xi})^2} (32 + 156\sqrt{\xi} + 232\xi + 187\xi^{3/2} + 82\xi^2 + 15\xi^{5/2})I_0^{L_+}(0)$$

$$- \frac{16}{v^4} (1 + 2\sqrt{\xi} - 2\xi)I_{1-}^{L_+}(0) - 16(1 + \sqrt{\xi})^4 I_{1+}^{L_+}(0)$$

$$+ \frac{\xi}{2(1-\sqrt{\xi})^2} (4 - 24\sqrt{\xi} + 5\xi + 10\xi^{3/2} + \xi^2)(I_{t-}^{L_+}(0) + I_{t+}^{L_+}(0))$$

$$+ \frac{\xi}{2(1+\sqrt{\xi})^2} (12 + 32\sqrt{\xi} - 15\xi - 18\xi^{3/2} + 5\xi^2)I_0^{L_0}(0)$$

$$\left. + \frac{(1-\sqrt{\xi})\xi}{(1+\sqrt{\xi})^2} (4 + 20\sqrt{\xi} + \xi - 9\xi^{3/2})I_{1-}^{L_0}(0) - \xi((2-\xi)(\hat{I}_{t-}^{L_0}(0) + I_{t+}^{L_0}(0)) - 4v(\ell_0^- + \ell_0^+)) \right], \tag{B38}$$

$$\rho_{43F}^{ll} = -8N\pi v\xi, \tag{B39}$$

$$\rho_{44F}^{ll} = N \left[-\frac{4}{1+\sqrt{\xi}} (8 + 12\sqrt{\xi} + 20\xi - 9\xi^{3/2} - 7\xi^2) + \frac{4}{v^2} (4 + 28\xi + 8\xi^{3/2} - 11\xi^2 - 5\xi^{5/2})\ell_1 \right.$$

$$+ \frac{2}{1-\sqrt{\xi}} (24 + 8\sqrt{\xi} - 6\xi + 14\xi^{3/2} - \xi^2 - 3\xi^{5/2})\ell_2$$

$$+ \frac{2v}{(1+\sqrt{\xi})^2} (8 + 16\sqrt{\xi} + 58\xi + 66\xi^{3/2} + 31\xi^2 + 6\xi^{5/2})\ell_3$$

$$- \frac{\sqrt{\xi}}{(1+\sqrt{\xi})^2} (32 + 36\sqrt{\xi} - 8\xi - 46\xi^{3/2} - 32\xi^2 - 7\xi^{5/2})I_0^{L_+}(0)$$

$$+ \frac{2v\sqrt{\xi}}{(1-\sqrt{\xi})^2} (8 - 6\sqrt{\xi} + 2\xi^{3/2} - \xi^2)(I_{t-}^{L_+}(0) - I_{t+}^{L_+}(0))$$

$$- \frac{1}{(1+\sqrt{\xi})^2} (16 + 32\sqrt{\xi} + 40\xi + 28\xi^{3/2} + 34\xi^2 + 28\xi^{5/2} + 7\xi^3)I_0^{L_0}(0)$$

$$\left. + 8v((2-\xi)(\hat{I}_{t-}^{L_0}(0) - I_{t+}^{L_0}(0)) - 4v\ell_0^-) \right]. \tag{B40}$$

[1] M. E. Peskin, in *Physics and Experiments at Linear Colliders,* edited by R. Orava, P. Eeorla, and M. Nordberg (World Scientific, Singapore, 1992).

[2] G. A. Ladinsky and C. P. Yuan, Phys. Rev. D **49**, 4415 (1994).

[3] T. L. Barklow and C. R. Schmidt, in *DPF '94: The Albuquerque Meeting,* edited by S. Seidel (World Scientific, Singapore, 1995).

[4] C. R. Schmidt, Phys. Rev. D **54**, 3250 (1996).

[5] J. G. Körner and M. C. Mauser, Lect. Notes Phys. **647**, 212 (2004).

[6] G. Mahlon and S. J. Parke, Phys. Rev. D **53**, 4886 (1996).

[7] G. Aad *et al.* (ATLAS Collaboration), Phys. Rev. Lett. **108**, 212001 (2012).

[8] J. G. Körner, A. Pilaftsis, and M. M. Tung, Z. Phys. C **63**, 575 (1994).

[9] M. M. Tung, Phys. Rev. D **52**, 1353 (1995).

[10] M. M. Tung, J. Bernabeu, and J. Peñarrocha, Nucl. Phys. **B470**, 41 (1996).

[11] S. Groote, J. G. Körner, and M. M. Tung, Z. Phys. C **70**, 281 (1996).

[12] S. Groote, J. G. Körner, and M. M. Tung, Z. Phys. C **74**, 615 (1997).

[13] S. Groote and J. G. Körner, Z. Phys. C **72**, 255 (1996); Eur. J. Phys. C **70**, 531(E) (2010).

[14] M. M. Tung, J. Bernabeu, and J. Peñarrocha, Phys. Lett. B **418**, 181 (1998).

[15] S. Groote, J. G. Körner, and J. A. Leyva, Phys. Lett. B **418**, 192 (1998).

[16] S. Groote, J. G. Körner, and J. A. Leyva, Eur. Phys. J. C **63**, 391 (2009).

[17] A. Brandenburg, M. Flesch, and P. Uwer, Phys. Rev. D **59**, 014001 (1998).

[18] A. Brandenburg, M. Flesch, and P. Uwer, Czech. J. Phys. **50**, 51 (2000).

[19] S. J. Parke and Y. Shadmi, Phys. Lett. B **387**, 199 (1996).

[20] J. Kodaira, T. Nasuno, and S. J. Parke, Phys. Rev. D **59**, 014023 (1998).

[21] S. Groote, J. G. Körner, and J. A. Leyva, Nucl. Phys. **B527**, 3 (1998).

[22] M. M. Tung and L. Jódar, Appl. Math. Lett. **19**, 775 (2006).

[23] L. Kaldamäe, S. Groote, and J. G. Körner, (to be published).

[24] B. Grzadkowski and Z. Hioki, Nucl. Phys. **B585**, 3 (2000); **B894**, 585(E) (2015).

[25] P. H. Khiem, E. Kou, Y. Kurihara, and F. L. Diberder, arXiv:1503.04247.

[26] W. Bernreuther, A. Brandenburg, Z. G. Si, and P. Uwer, Nucl. Phys. **B690**, 81 (2004).

[27] W. Bernreuther, A. Brandenburg, Z. G. Si, and P. Uwer, Phys. Rev. Lett. **87**, 242002 (2001).

[28] W. Bernreuther and Z. G. Si, Nucl. Phys. **B837**, 90 (2010).

[29] W. Bernreuther, D. Heisler, and Z. G. Si, J. High Energy Phys. 12 (2015) 026.

[30] S. Groote, J. G. Körner, B. Melić, and S. Prelovsek, Phys. Rev. D **83**, 054018 (2011).

[31] M. Fischer, S. Groote, J. G. Körner, M. C. Mauser, and B. Lampe, Phys. Lett. B **451**, 406 (1999).

[32] M. Fischer, S. Groote, J. G. Körner, and M. C. Mauser, Phys. Rev. D **65**, 054036 (2002).

[33] A. Czarnecki, J. G. Körner, and J. H. Piclum, Phys. Rev. D **81**, 111503 (2010).

[34] S. Groote, W. S. Huo, A. Kadeer, and J. G. Körner, Phys. Rev. D **76**, 014012 (2007).

[35] A. Czarnecki, M. Jeżabek, and J. H. Kühn, Nucl. Phys. **B351**, 70 (1991).

[36] A. Czarnecki, M. Jeżabek, J. G. Körner, and J. H. Kühn, Phys. Rev. Lett. **73**, 384 (1994).

[37] A. Czarnecki and M. Jeżabek, Nucl. Phys. **B427**, 3 (1994).

[38] J. G. Körner and D. Pirjol, Phys. Rev. D **60**, 014021 (1999).

[39] S. Groote and J. G. Körner, Phys. Rev. D **80**, 034001 (2009).

[40] K. A. Olive *et al.* (Particle Data Group Collaboration), Chin. Phys. C **38**, 090001 (2014).